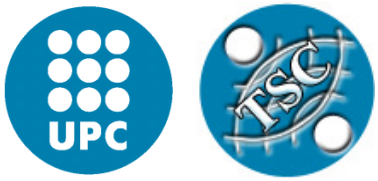

Feasibility Study on SAR Systems on Small Satellites

by
Albert García Mondéjar

Paco López Dekker, Project Advisor

Barcelona, January 2009

ACKNOWLEDGEMENTS

This project would not have been possible without the academic and moral support of a large number of people.

My first debt of gratitude is to Paco, my tutor and also a very good friend. I would like to thank the teachers from TSC for having taught me all these interesting courses in which I have taken part.

A special thank to my family and friends for his enormous support during these years of degree. I would like to emphasize people from A.C Telecogresca for letting me be part of this big family.

I do not want to finish without mentioning my girlfriend Senda. She has been the most important person in the last year and she always tries to help me. Thanks a lot for these beautiful moments.

CONTENTS

1 INTRODUCTION

1.1 Global Context of SAR Remote Sensing

Remote sensing is the group of techniques that allow us to acquire information of objects or phenomenon's, without the necessity of being in contact with the object (such as by way of aircraft, spacecraft, satellite, or ship). Remote sensing is the collection through the use of a variety of remote devices of information on an interesting object or area. Nowadays, when we talk about remote sensing, it generally means the use of imaging sensor technologies including the use of aircraft and spacecraft boarded instruments, and it is distinct from other imaging-related fields such as medical imaging.

There are two classes of remote sensing systems. Passive sensors detect natural radiation that is emitted or reflected by the object or the area being observed. Reflected sunlight is the most common source of radiation measured by passive sensors. Examples of passive remote sensors include film photography, infra-red, charge-coupled devices, and radiometers.

On the other hand, active sensors emit energy with the intention to scan objects and areas. Imaging radar (RAdio Detection And Ranging) is an example of active remote sensing and has become an alternative technique for observing the Earth from space.

Radar provides its own energy source and, therefore, can operate either day or night and through cloud cover. This means that Radar technology can provide day-and-night imagery of the Earth independently of weather conditions

A radar system has three primary functions:

- It transmits a microwave signal (from a frequency of 0.3 GHz to 300 GHz) towards a scene.
- It receives the portion of the transmitted energy backscattered from the scene.
- It observes the strength (detection) and the time delay (ranging) of the returned signals

A SAR, Synthetic Aperture Radar, is a coherent radar system that can generate high-resolution images. Signal processing uses magnitude and phase of the received signals over successive pulses to create the image.

A synthetic aperture is produced by signal processing. The aperture has the effect of lengthening the antenna, as the line of sight direction changes along the radar platform trajectory.

The achievable azimuth resolution of a SAR is approximately equal to one-half the antenna length and does not depend on platform altitude. High range resolution is achieved through pulse compression techniques. With the aim of mapping the ground surface the radar beam

is directed to the side of the platform trajectory; with a antenna beam wide enough in the along-track direction, an identical target or area may be illuminated a number of times without a change in the antenna look angle.

Remote sensing sensors can be carried on a variety of platforms to view and image targets. Satellites provide a large fraction of the remote sensing imagery. They have several unique characteristics which make them very useful for observing the Earth's surface. Remote sensing satellites are designed to follow an orbit which, in conjunction with the Earth's rotation, allows them to cover most of the Earth's surface over a certain period of time. The area imaged on the surface, is referred to as the swath. Imaging swaths for space-borne sensors generally vary between tens and hundreds of kilometers wide.

Sensors on satellites generally can "see" a much larger area of the Earth's surface than would be possible from a sensor onboard an aircraft. Also, because they are continually orbiting the Earth, it is relatively easy to collect imagery on a systematic and repetitive basis in order to monitor changes over time.

The geometry of orbiting satellites can be calculated accurately and facilitates correction of remote sensing images to their correct geographic orientation and position. However, aircraft sensors can collect data at any time and over any portion of the Earth's surface while satellite sensors are restricted to collecting data over only those areas and during specific times dictated by their particular orbits.

Satellite orbits are matched to the capability and objective of the sensor(s) they carry. Orbit selection can vary in terms of altitude (their height above the Earth's surface) and their orientation and rotation relative to the Earth.

1.1.1 History of SAR space missions

Since the first launch of a SAR satellite many other missions have been planned. In the last five years many research centers have been planning the development of small platforms that were able to carry SAR systems. The reduction in the orbit altitude helps to reduce costs and the delivery time of new data information.

Table 1.1 summarizes the most important parameters of the recent space-borne SAR missions. Values in blue were not available and have been simulated, calculated or assumed.

1.1.1.1 SEASAT, 1978

SEASAT was the first Earth satellite designed for remote sensing of the Earth's oceans and had onboard the first space-borne SAR. [1]

Mision	TerraSAR-X		MAPSAR			SAR on Proteus		SAR LUPE	SAR on Myriade	
Country	Germany		Brazil & Germany			France		Germany	France	
Modes	Strip map	Spotlight	Scansar	High - HR	Medium - MR	Low - LR	Strip Map	Scansar		Strip	Scansar and Spotlight
Orbital Altitude	514 km			600 - 650 km			500 km		500 km	470 Km	
Ground range resolution	1.55 – 3.21 m (1,86)	1.34m - 3.21m	1.55 m - 3.21 m	4,7 - 3,1 m	10 m	20 m	3m	-	1 m	-	-
Azimuth resolution	2,4m at 150 and 300 MHz	1 m and 2 m (single pol)	16 m	3,1 m	10 m	20 m	1,87 m	-	1 m	2 m	5m
Swath	30 km (single pol.) 15 km (double pol.)	10km	100 km	38,3 - 20,5 km	45,1 - 35 km	43,4 - 28 km	25 km	125 km	240,15 km	3 km	10 km
NEσ^0	-22dB	-23dB	-21dB	-23.6 -19dB	-28.9 - 25.4 dB	-34.6 -33.3 dB	-20dB			17 dB	24 dB
Incidence angle	20° - 45°	20° - 55°	20° - 45°	20,3 º - 47,6 º	20 º - 48,1 º	20 º - 36,8 º	15º - 46 º		21º - 57º	50º	40º
Antenna Type	Active planar array antenna			Cassegrain configuration elliptical			rectangular		elliptical parabolic reflector	circular parabolic reflector	
Antenna length (azimuth)	4.8 m			7.5 m			1,87*2 m		3.3 m	2.4 m diameter	
Antenna width (elevation)	0.7 m			5 m			1,87 m		2.7 m		
Radiation efficiency	0,5			0,707			0,707		0,707	0,707	
Aperture efficiency	0,5			0,5			0,5		0,5	0,5	
Average Power	360 W (Pmax*duty cycle)			67,95W	67 W	106.4 W	50,697 W		250 W	300 *0.2W	
PRF	2.0 kHz – 6.5 kHz			2650-2718 Hz	2660-2680 Hz	5320 Hz	4 KHz		5 khz	3,175 KHz	
f_0	9,65 GHz (X band)			1,3 GHZ (L band)			9,65 GHz (X band)		9,65 GHz (X band)	9,65 GHz (X band)	
Payload Mass	394 kg			280 Kg			300 kg		-	47 kg	
Satellite Mass	1023 kg			532 kg			700 kg		770 kg	120 kg	
max unambiguous swath width	78,8903 km	78,8903 km	631,122 km	123,261 km	397,615 km	795230 km	73,6874 km		39,4051 km	78,638 km	196,595 km
Antenna gain	42,6015 dB	42,6015 dB	51,6324 dB	35,6319 dB	40,7182 dB	43,7285 dB	46,5771 dB		45,4539 dB	41,0979 dB	41,0828 dB
NEσ^0	-25,4355 dB			-23,7704 dB	-33,9758dB	-49,010 dB	- 20 dB		- 19,9120 dB	-22,7886 dB	-22,7584 dB
Power Average	91,3207 W	205,472 W	2,02568 W	65,3349 W	8,29723 W	3,35616 W	50,697 W		255,119 W	79,1148 W	399,284 W

Table 1.1 SAR parameters summary and performance simulation results

Fig. 1.1 Seasat image made with the digital correlator of waves off Alaska's southern coastline near Yakutat (note the glaciers on land)

The mission was designed to demonstrate the feasibility of global satellite monitoring of oceanographic phenomena and to help determine the requirements for an operational ocean remote sensing satellite system.

Specific objectives were to collect data on sea-surface winds, sea-surface temperatures, wave heights, internal waves, atmospheric water, sea ice features and ocean topography, Fig. *1.1*. Seasat was managed by NASA's Jet Propulsion Laboratory and was launched on 28 June 1978 into a nearly circular 800 km orbit with an inclination of 108°. Seasat operated for 105 days until 10 October 1978, when a massive short circuit in the satellite's electrical system ended the mission.

SEASAT was able to detect the wakes of submerged submarines, a discovery not anticipated before launch. The conspiracy theory holds that once this was discovered, the military shut SEASAT down, with a cover story of a power supply short.

1.1.1.2 SIR-A, 1981

The Shuttle Imaging Radar A (SIR-A) was launched aboard the space shuttle Columbia in November 12, 1981 on shuttle orbital flight test -2 (OFT-2) [2]. It formed part of NASA's Office of Space and Terrestrial Applications (OSTA-1) payload.

The main goal of SIR-A was to further our understanding of radar signatures of geologic features; a secondary goal was to assess the shuttle as a scientific platform for Earth

observations. The satellite altitude was 265 km and operates in L-Band (frequency of 1.275 GHz).

1.1.1.3 SIR-B, 1982

Shuttle Imaging Radar B (SIR-B) was the second major step in the evolutionary NASA radar remote sensing research program. [3]

The radar imagery collected at the fixed look angle SEASAT and SIR-A experiments demonstrated the relationship between image intensity and the incidence angle of the radar at the surface. This led to the design of SIR-B, the first space-borne SAR with a mechanically tiltable antenna. This allowed the acquisition of multi-incidence angle imagery.

SIR-B was launched on October 5, 1984 aboard the Space Shuttle Challenger on flight 41-G into a nominally circular orbit. The average altitude for the first 20 orbits was 360 km; for the next 29 orbits was 257 km; and for the duration of the mission 224 km. At the 224 km altitude, the orbit was allowed to drift slightly westward with an approximate 1- day repeat cycle. This enabled SIR-B to image a given site at several different incidence angles on subsequent days over the course of the mission.

1.1.1.4 Magellan, 1989

The Magellan spacecraft, named after the sixteenth-century Portuguese explorer whose expedition first circumnavigated the Earth, was launched May 4, 1989, and arrived at Venus on August 10, 1990. [4]

Magellan's solid rocket motor placed it into a near-polar elliptical orbit around the planet. During the first 8-month mapping cycle around Venus, Magellan collected radar images of 84 percent of the planet's surface, with resolution 10 times better than that of the earlier Soviet Venera 15 and 16 missions. Altimetry and radiometry data also measured the surface topography and electrical characteristics.

1.1.1.5 ERS-1, 1991

European Remote Sensing satellite (ERS-1) was the first European Space Agency's Earth-observing satellite. It was launched on July 17, 1991 into a Sun synchronous polar orbit at a height of 782–785 km.[5]

It carried a comprehensive payload including an imaging SAR (operating in C band), a radar altimeter and other powerful instruments to measure ocean surface temperature and winds at sea.[6]

1.1.1.6 J-ERS-1, 1992

JERS-1, launched in Feb 1992 and finalized in Oct 1998, was a joint Japanese radar/optical mission with NASDA/JAXA lead. [7]

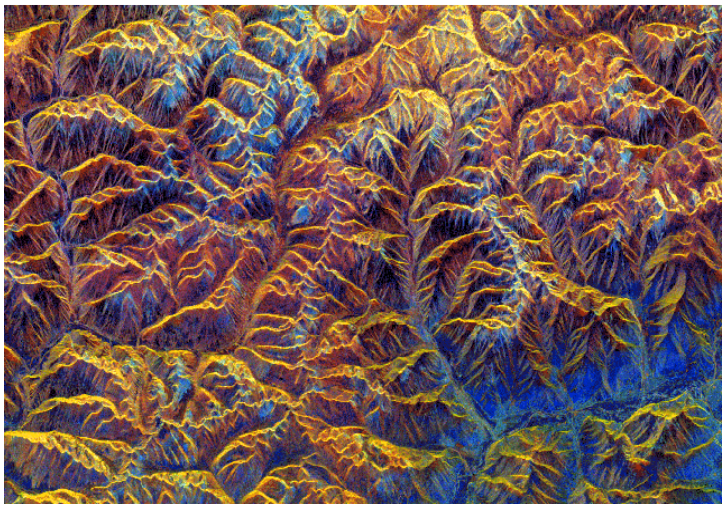

Fig. 1.2 SIR-C Image of the southeast Tibet, about 90 kilometers (56 miles) east of the city of LhasaMay 14, 1998

The overall objectives were the generation of global data sets with SAR and OPS sensors aimed at surveying resources, establishing an integrated Earth observation system, verifying instrument/system performances. The mission applications focused on survey of geological phenomena, land usage, observation of coastal regions, geologic maps, environment and disaster monitoring and demonstration of two-pass SAR interferometry for change detection.

1.1.1.7 SIR-C/X-SAR, 1994

SIR-C/X-SAR stands for space-borne Imaging Radar-C/X-band Synthetic Aperture Radar.[8]

SIR-C/X-SAR is an imaging radar system scheduled for launch aboard the NASA Space Shuttle in 1994. It consists of a radar antenna structure and associated radar system hardware that is designed to fit inside the Space Shuttle's cargo bay. On take-off, the cargo bay doors are closed as seen in the graphic on the next page. After the Space Shuttle has reached a stable Earth orbit, the cargo bay doors will be opened, the antenna structure will be deployed, and SIR-C/X-SAR will be switched on, to begin using its state-of-the-art radar technology to image the earth's surface. Radar images, Fig. 1.2, generated by SIR-C/X-SAR will be used by scientists to help understand some of the processes which affect the earth's environment, such as deforestation in the Amazon, desertification south of the Sahara, and soil moisture retention in the Mid-West.

1.1.1.8 ERS-2, 1995

ERS-2, was launched on April 21, 1995, on an Ariane 4, from ESA's Guiana Space Centre near Kourou, French Guiana. [9]

In 2001, after the failure of several on-board gyro systems, an innovative new scheme for flying and controlling the ERS-2 mission without gyros was invented by a group of engineers across ESA and industry- the "gyro-less" yaw steering mode or "Zero-Gyro Mode". In 2003, a failure in the on-board data storage system led to the mission being re-designed as "real-time" only, with science data directly relayed to ground at the time of

acquisition. These in-flight adaptations have enabled the mission to be extended well beyond its design lifetime, and recently led ERS-2 to celebrate its 60,000th orbit.

1.1.1.9 RADARSAT-1, 1995

RADARSAT-1 is Canada's first commercial Earth observation satellite. It was launched at 14h22 UTC on November 4, 1995 from Vandenberg AFB in California, into a sun-synchronous orbit (dawn-dusk) above the Earth with an altitude of 798 kilometers and inclination of 98.6 degrees. [10]

Developed under the management of the Canadian Space Agency (CSA) in cooperation with Canadian provincial governments and the private sector, it provides images of the Earth for both scientific and commercial applications. RADARSAT-1's images are useful in many fields, including agriculture, cartography, hydrology, forestry, oceanography, geology, ice and ocean monitoring, arctic surveillance, and detecting ocean oil slicks.

1.1.1.10 Shuttle Radar Topography Mission, 2000

SRTM (Shuttle Radar Topography Mission) is an international project spearheaded by the National Geospatial-Intelligence Agency (NGA) and the National Aeronautics and Space Administration (NASA). [11]

The SRTM obtained elevation data on a near-global scale to generate the most complete high-resolution digital topographic database of Earth. SRTM consisted of a specially modified radar system that flew onboard the Space Shuttle Endeavour during an 11-day mission in February of 2000.

1.1.1.11 ENVISAT, 2002

Envisat (Environmental Satellite, Fig. 1.3) is an Earth-observing satellite built by the European Space Agency. It was launched on the 1st March 2002 aboard an Ariane 5 into a Sun synchronous polar orbit at a height of 790 km (±10 km). It orbits the Earth in about 101 minutes with a repeat cycle of 35 days. [12]

Envisat carries an array of nine Earth-observation instruments that gather information about the earth (land, water, ice, and atmosphere) using a variety of measurement principles.

Several of the instruments are advanced versions of instruments that were flown on the earlier ERS-1 and ERS-2 missions and other satellites.

- ASAR (Advanced SAR) operating in C band can detect changes in surface heights with sub-millimeter precision.
- MERIS (MEdium Resolution Imaging Spectrometer) measures the reflectance of the Earth (surface and atmosphere) in the solar spectral range (390 to 1040 nm) and transmits 15 spectral bands back to the ground segment.
- AATSR (Advanced Along Track Scanning Radiometer) can measure the temperature of the sea surface

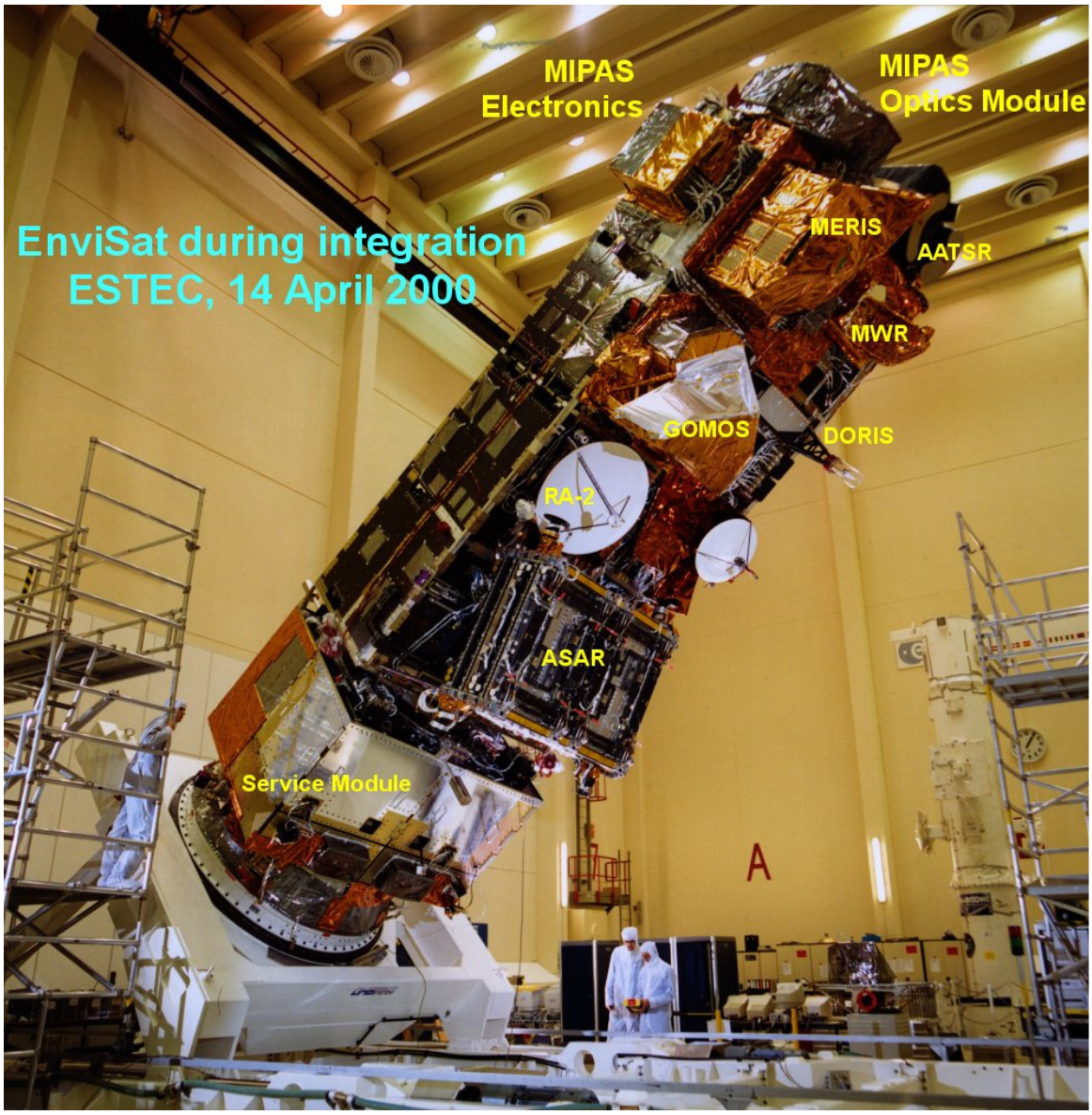

Fig. 1.3 Envisat during integration, 14 April 2000

- RA-2 (Radar Altimeter 2) is a dual-frequency Nadir pointing Radar operating in the K_u band and S bands, it is used to define ocean topography, map/monitor sea ice and measure land heights.
- MWR (Microwave Radiometer) for measuring water vapour in the atmosphere and estimate the tropospheric delay for the Altimeter
- DORIS (Doppler Orbitography and Radiopositioning Integrated by Satellite) for orbit determination to within 10 cm or less
- GOMOS (Global Ozone Monitoring by Occultation of Stars) looks to stars as they descend through the Earth's atmosphere and change color, which also tells a lot about the presence of gases such as O_3 (ozone), and allows for the first time a space-based measurement of the vertical distribution of these trace gases.
- MIPAS (Michelson Interferometer for Passive Atmospheric Sounding) is a spectrometer
- SCIAMACHY (SCanning Imaging Absorption spectroMeter for Atmospheric CHartographY) compares light coming from the sun to light reflected by the Earth, which provides information on the atmosphere through which the earth-reflected light has passed.

1.1.1.12 ALOS, 2006

Advanced Land Observation Satellite (ALOS), a Japanese satellite, was launched from Tanegashima Island, Japan on January 24, 2006 by a H-IIA rocket. Weather and sensor problems have caused launch delays. [13]

ALOS has been developed to contribute to the fields of mapping, precise regional land coverage observation, disaster monitoring, and resource surveying. It enhances land observation technologies acquired through the development and operation of its predecessors, the Japanese Earth Resource Satellite-1 (JERS-1, or Fuyo) and the Advanced Earth Observing Satellite (ADEOS, or Midori).

ALOS has three sensors onboard: the Panchromatic Remote-sensing Instrument for Stereo Mapping (PRISM), which is comprised of three sets of optical systems to measure precise land elevation; the Advanced Visible and Near Infrared Radiometer type 2 (AVNIR-2), which observes what covers land surfaces; and the Phased Array type L-band Synthetic Aperture Radar (PALSAR), which enables day-and-night and all-weather land observation.

1.1.1.13 TerraSAR-X, 2007

TerraSAR-X is a German remote sensing satellite program which is the first commercially available radar satellite to offer one meter resolution [14][15].

TerraSAR-X is the first satellite ever to be built in a Public Private Partnership (PPP) in Germany. In this partnership, the Federal Republic of Germany, represented by the German Aerospace Center (DLR), and Europe's leading satellite company ASTRIUM GmbH have agreed to jointly bear the costs of constructing and implementing this X-band radar satellite.

In order to ensure the commercial success of the mission, ASTRIUM GmbH founded its 100% subsidiary Infoterra GmbH in 2001; the company being responsible for establishing a commercial market for TerraSAR-X data as well as TerraSAR-X-based geoinformation products and services.

1.1.1.14 RADARSAT-2, 2007

RADARSAT-2 is an Earth observation satellite that was successfully launched December 14, 2007 for the Canadian Space Agency by Starsem, using a Soyuz FG launch vehicle, from Kazakhstan's Baikonur Cosmodrome. RADARSAT-2 was previously assembled, integrated and tested at the David Florida Laboratory near Ottawa, Ontario before the start of its launch campaign. [16]

The Satellite has SAR sensor with multiple polarization modes. Its highest resolution will be 3 m in Ultra Fine mode with 100 m positional accuracy. Its left looking capability allow the spacecraft the unique capability to image the Antarctic on a routine basis providing data in support of scientific research.

RADARSAT-2 is based on RADARSAT-1. It has the same orbit (798 km altitude sun-synchronous orbit with 6 p.m. ascending node and 6 a.m. descending node). RADARSAT-2 is separated by half an orbit period (~50 min) from RADARSAT-1 (in terms of ground track it would represent ~12 days ground track separation). It is filling a wide variety of roles, including sea ice mapping and ship routing, iceberg detection, agricultural crop monitoring, marine surveillance for ship and pollution detection, terrestrial defense surveillance and target identification, geological mapping, land use mapping, wetlands mapping, topographic mapping.

1.1.1.15 SAR-LUPE, 2007

SAR-Lupe is a SAR reconnaissance satellite imaging project of the German government, in particular the German Ministry of Defense (BMVg) and the Federal Office of Defense

Technology and Procurement, referred to as BWB (Bundesamt für Wehrtechnik und Beschaffung), Koblenz, Germany (BWB manages the procurement of the ground and space segments). The overall objective is to provide high-resolution radar imagery to German defense forces over a period of ten years starting in 2005. SAR-Lupe is in fact the first dedicated reconnaissance satellite imaging project of Germany [17][18][19].

1.1.1.16 JianBing 5 (YaoGan WeiXing 1/3), 2007

A new satellite named Remote Sensing Satellite 1 (or YaoGan WeiXing-1 in its Chinese translation) was successfully launched on 12 Nov 2007 by a CZ-4B (Batch-02) launch vehicle from Taiyuan Satellite Launch Centre (TSLC). While the report about the purposes and technical details of the satellites was very brief, it is understood that this 2,700 kg satellite was in fact China's first space-based SAR system, with a military designation JianBing (JB-5) [20].

1.1.1.17 SURVEYOR, 2007

A unique and entirely commercial "Surveyor" SAR satellite constellation comprising 5 low-cost medium C Band sensors has been placed under a global design competition by the Beijing-China sited company Tuyuan Technologies was launched in 2007 [21][22].

1.1.1.18 KOMPSAT-5, 2010

The goal of the KOMPSAT-5 (Korean Multi-purpose Satellite 5) project is to lead the development of the first Korean SAR Satellite using manpower and facilities from the KOMPSAT-3 program. It aims to support the national SAR satellite demand and form a technology infrastructure to make inroads into the world space industry [23].

KOMPSAT-5, which started in the middle of 2005, will be launched in 2010 and its payload will be an X-band SAR and it will operate at Dawn-Dusk orbit between 500km to 600km of altitude.

1.1.1.19 ASTROSAR-LITE, 2010

The AstroSAR-Lite satellite, pioneered by Astrium, provides an innovative, agile,

affordable space SAR system focused to provide unprecedented revisit and coverage with high resolution for the regional user in the tropics and sub-tropics. AstroSAR-Lite is optimised to maritime, environmental, security and disaster monitoring applications.

The baseline satellite operates in various modes to obtain images ranging from 10 km x 1,000 km at three-metre resolution, up to 100 km x 1,000 km at 20–30 metre resolutions over the 'footprints' of each of several regional users.

Mechanical steering of the whole satellite provides major beam pointing of ±45°, enabling access to both left and right sides, augmenting and simplifying the electronic beam steering thus minimizing cost of the expensive TR modules that are typical of other active phased array systems.

Under a new initiative, AstroSAR-Lite customers have the option to join the AstroSAR Lite Club – a shared constellation – effectively securing the use of several satellites for the price of one.

1.1.1.20 SENTINEL,2011

The Sentinel-1 series of satellites will address the issue of data continuity for SAR data at large. The immediate priority is to ensure such continuity for C-band data [25].

Under the current scenario, provision of ENVISAT data to feed SAR-based services is likely to cease in the 20011-2013 timeframe. In order to meet the need for continuity, and taking into account the availability of Radarsat-2, the first Sentinel 1 satellite should be launched before the end of the Envisat operations.

The experience with ERS, Envisat and Radarsat constitutes the basis for the Sentinel-1 mission requirements and concept.

1.1.1.21 MAPSAR, 2013

The initiative of the joint study of a small space-borne SAR (MAPSAR) is a consequence of a long-term Brazilian-German scientific and technical cooperation that was initiated between INPE and DLR in the 1970s. The decision to perform a pre-phase "A" study for MAPSAR was established in 2001 following several meetings in both agencies. Based on the specific and complementary experience of both partners, the sharing of the thematic responsibilities within the study was agreed. Brazil is responsible for the platform and integrated satellite analysis and Germany for the payload and orbit analysis [26]

1.1.1.22 SAR on Proteus, launch not scheduled

PROTEUS is a French acronym standing for "Plateforme Reconfigurable pour I'Observation, les TElecommunications et les Usages Scientifiques" (Reconfigurable Platform for Observation, Communications and Scientific Applications) [27].
A SAR mission on the Proteus platform is being studied, the main objectives for this SAR

mission concentrate in three areas:

- Accommodation due to the relatively large SAR antenna size
- Power and distribution in view of the critical requirements associated with the SAR transmission
- Command / Control, due to the relatively large amount of data required to program the SAR payload

1.1.1.23 SAR on Myriade, launch not scheduled

The Myrlade bus is already considered for the interferometric Cartweel (ICW') mission promoted by CNES. ICW aims at providing medium resolution DTM (Digital Terrain Model) with several passive Microsar which receive the Radar echoes issued from the transmission of a conventional SAR satellite being used as a source of opportunity. In addition a small monostatic SAR mission is also under study [28].

1.1.2 ICC, PCOT and SARMISP

The aim of the "Institut Cartogràfic de Catalunya" (ICC), the official mapping agency of Catalonia, is to remain in the leading edge of the mapping technologies. For a mapping agency the benefits of satellite imagery are clear and include rapid acquisition of data covering large areas.

The PCOT, the Catalan Earth Observation Program, is an ICC strategic program to boost activities, products, and Earth Observation services. The aims of PCOT are:

- Promote the interest in the field of space technology in Catalonia.
- Encourage, improve and enlarge the participation of the Institute Cartographic of Catalonia in the design, development and operation of small satellite missions for Earth observation
- Team up with other mapping agencies doing similar projects.
- Allow public and private national end user's and stakeholders, in different fields and at different levels, to have access to satellite information.
- Develop design methodologies and processes to translate data into useful mapping information.
- Encourage new design ideas on satellite payload, satellite services, and satellite constellations.

Whithin the PCOT projects, the ICC contracted a feasibility study to the Microwave Remote Sensing group, which belongs to the Signal theory and Communications Department of the Universitat Politècnica de Catalunya (UPC), to determine the state of the art, main constraints and future developments in this field and to make recommendations for a possible space-related initiative. This study is called SARMISP, SAR Mission on Small Platforms.[29]

This final career project has been developed in the context of SARMISP and its first results have been presented in the 2on Workshop PCOT on Radar Earth Observation.

1.2 Purpose and limitations of the project

The design of an orbital SAR mission is the result of a number of trade-offs. For example, a higher resolution requires more transmitted power, or an increase in the strip-map azimuth resolution results in a smaller possible swath. In the following sections the most relevant parameters of a SAR system are discussed and the inter-relation between different parameters is explored.

It is important to emphasize right away that the most critical trade-offs are not technological but are, instead, fundamental in nature. For example, while the transmitted power may be increased through technological improvement, the dimensions of an antenna, given some basic specifications, are lower bounded by first principles.

It is also worth noting that the scope of this study is limited to currently operational SAR configurations, as the goal of this project is to evaluate the feasibility of an operational SAR mission on a compact platform, and not to propose novel SAR concepts. Where necessary in our analysis we have chosen the option most compatible with the nature of a small mission. For example, within the margin of possible orbital altitudes, the lower range is assumed since it reduces the required power.

1.3 Document Content

A brief introduction of this document contents is given next.

Chapter 2 discusses the SAR systems parameters that have to be considered in the design of the mission. Chapter 3 presents the design flow established in order to design a SAR mission with the parameters considered in chapter 2. Chapter 4 shows a description of the software implemented. A SAR compact mission proposal is detailed in chapter 5. Applications of interest, satellite orbit, sensor design and satellite down link are the main points of the mission designed. The summary, conclusions and future lines are discussed in chapter 6.

2 SAR SYSTEM CONSIDERATIONS

The design of SAR system is generally dependent on the application for which it is intended. Typically, the specifications are provided to the design engineer by the end-user include:

- Ground range and azimuth resolution.
- Incidence angle.
- Desired swath width.
- Wavelength.
- Polarization.
- Sensitivity, which is usually expressed in as a noise equivalent σ_0.
- Radiometric accuracy; SNR.

Additional constraints are imposed by the available platform resources and overall mission design: payload mass, available power and physical dimensions; platform altitude; ephemeris/attitude determination accuracy; attitude control; downlink data rate, and so on. It is worth noting that these constraints impose fundamental limitations to the achievable performance of the resulting SAR system. For example:

- Mass and size limitations upper bound the antenna area (A) and, therefore, limit also the antenna gain (G_t). This has an impact on sensitivity but also on the azimuth resolution and/or the achievable unambiguous swath.
- The maximum average radiated power (P_{avg}) is limited by the available DC power.

The final design is a result of an interactive procedure, trading-off conflicting requirements to achieve the optimal design.

2.1 Orbital SAR geometry

Fig. 2.1 and Fig. 2.2 illustrate the geometry of an orbital SAR system, showing the relationship between the incidence angle η and the look angle γ, for a smooth spherical geoid model. The spacecraft position is given by $h+R_{en}$ where R_{en} is the radius of the Earth at the nadir and h is the S/C altitude relative to the nadir point. The radar is on board an orbital platform moving a speed Vs in near circular orbit at constant altitude. The radar beam is pointed approximately in a perpendicular direction to the orbit and downwards at the surface of the flat earth.

2.1.1 Altitude (h)

Choosing the orbital altitude presents the first trade-off between a low orbit that, by being closer to the observed targets, reduces the power required by the radar and the need to minimize atmospheric friction, which increases at lower altitudes and translated to the need to carry more fuel (hydrazine) to maintain orbit. By examining recent missions such as TerraSAR-X or SARLUPE, an altitude of 500 km appears close enough to a practical

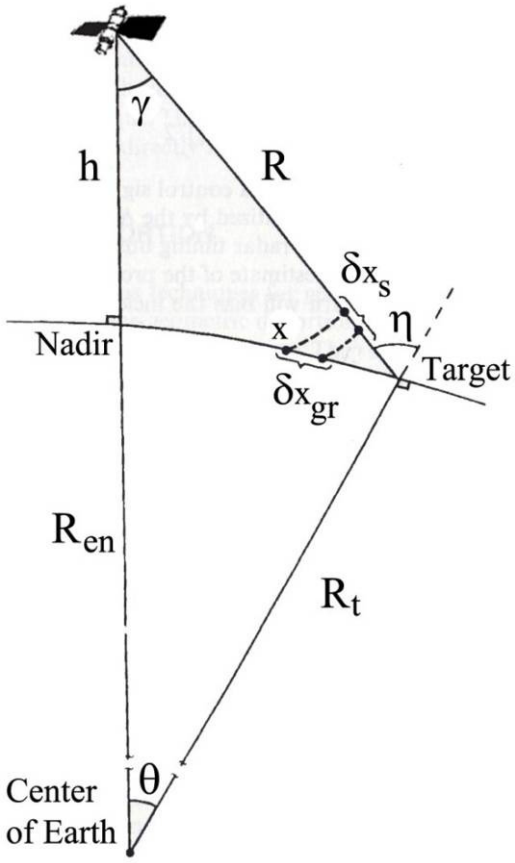

Fig. 2.1 System geometry considering a smooth geoid.

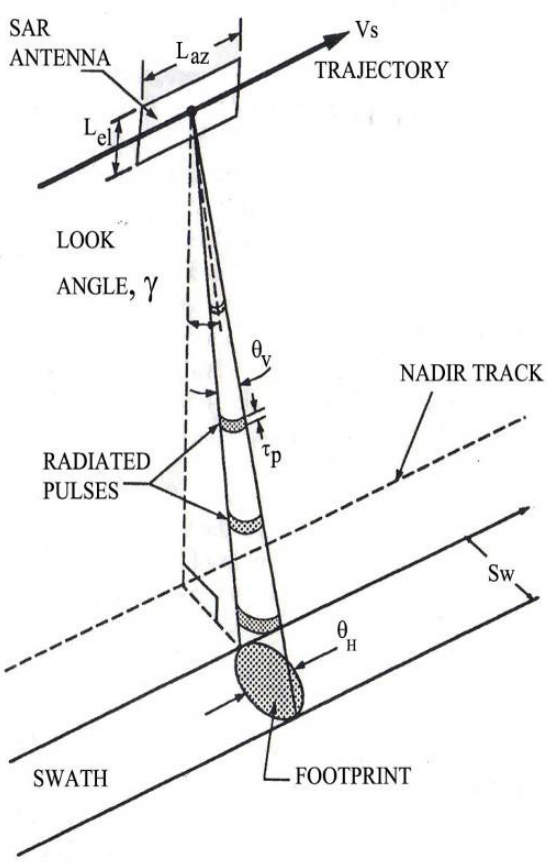

Fig. 2.2 Simplified geometry of a side-looking SAR

lower bound and will, therefore, be assumed throughout the rest of this chapter. As there are missions that work in altitudes around 500 Km we will consider this altitude our minimum altitude allowable.

The orbital velocity can be approximated by

$$V_s = \sqrt{\frac{G \cdot M_t}{R_t + h}}, \tag{2.1}$$

where G is the universal gravitational constant ($G \approx 6{,}67428 \times 10^{-11}$ m^3 kg^{-1} s^{-2}), M_t is the Earth mass ($Mt \approx 5{,}9736 \times 10^{24}$ kg), Rt is the Earht radius ($R_t \approx 6380$ km) and h is the satellite altitude. At 500 km height this gives an orbital velocity of approximately 7.6 km/s.

2.1.2 Incidence angle (η)

The incidence angle is the angle between the radar beam and the normal to the earth's surface at a particular point of interest. It is important because it affects the radar cross section of target area (in general, a smaller incidence angle results in more backscattered

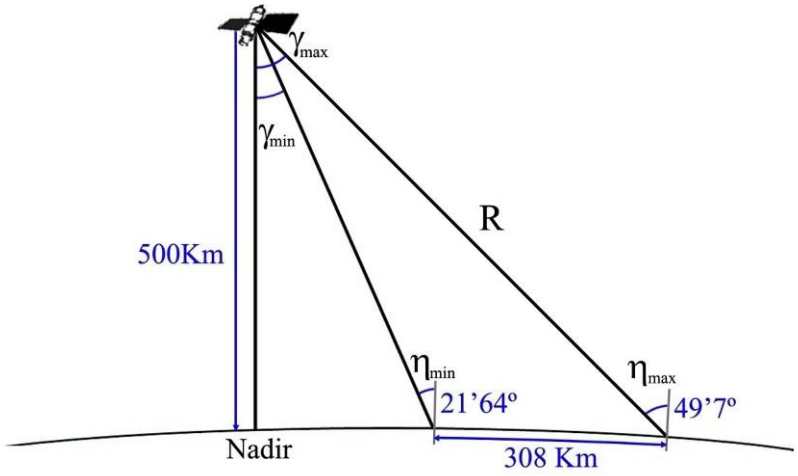

Fig. 2.3 Access region of the SAR sensor

	Minimum values	**Maximum values**
γ	20º	45º
η	21.64º	49.7º
R	532,13 Km	707,10 Km

Table 2.1: look angles, incidence angles and slant-range to targets

power) but also the ground range resolution (which improves for larger incidence angles) and the swath of the system.

Pointing the radar beam between γ_{min} and γ_{max}, the system must be able to cover a given area of interest. It is worth noting that by increasing the range of possible incidence angles it is possible to reduce the system's access time to any particular region of interest. The relation between the look angle and the incidence angle is given by

$$\eta = \sin^{-1}\left(\frac{(h+R_{en})\sin\gamma}{R_t}\right). \tag{2.2}$$

The starting values of the look angle haven been chosen from 20º to 45º so we were able to sight areas in 308 km with a single trace. We can calculate the range of incidence angles and the slant range distances. Table 2.1 shows a summary of the geometric parameters used in this report, which are further illustrated in Fig. 2.3.

2.2 Sensitivity: Radar Range Equation

One of the starting points for any radar design is the radar range equation, which relates the signal to noise (SNR) at the receiver with the target's radar cross-section, its distance to the

radar and a number of system parameters. The radar range equation (2.3) can be expressed in a number of ways. For a SAR system, a useful expression is the single look signal to noise, [30]

$$SNR_1 = \left(\frac{\eta_{ant} P_{avg} G_t^2 \lambda_0^3 \delta R_g \sigma_0}{2(4\pi)^3 R^3 (k_B T_{sys} V_s)} \right), \tag{2.3}$$

where η_{ant} is the radiation efficiency of the antenna, λ_0 is the carrier wavelength, δR_g is the ground range resolution, σ_0 is the normalized radar cross-section (radar cross-section per area unit), R is the range to the target, k_b is the Boltzmann constant, T_{sys} is the system equivalent noise temperature and V_s the velocity of the platform. It is worth noting that despite the strong dependence on the range, for orbital systems the range variation is small in relative terms and has a smaller impact than, for example, across-swath antenna gain variations.
The sensitivity is usually specified in terms of the noise equivalent $\sigma_{0,}$ which results from setting SNR=1 in (2.3), which yields [31]

$$\sigma_{0,ne} = \left(\frac{2(4\pi)^3 R^3 (k_B T_{sys} V_s)}{\eta_{ant} P_{avg} G_t^2 \lambda_0^3 \delta R_g} \right), \tag{2.4}$$

The sensitivity can be improved in several ways:

1. Increase the average power by increasing either the peak power, which is technology-limited, or the pulse duration. It is upper-bounded by the total available power.
2. Reduce the range to the target, which for an orbital case implies lowering the orbital altitude.
3. Increase the antenna gain, which implies increasing it physical size and either degrading the azimuth resolution or the swath width.
4. Reduce the required resolution.
5. Reduce the noise introduced by the system (either receiver noise or quantization noise). It is worth stressing that the noise power is lower bounded by the noise temperature of the antenna, which for a SAR system is usually in the order of 300K.
6. Reduce system losses by improving the antenna feed system (waveguide) or by inserting T/R modules into the feed to improve the system gain; again at the cost of increasing power consumption.

2.3 Resolution considerations.

2.3.1 Range Resolution

For a SAR system, the ground range resolution is given by [32]

$$\delta R_g = \frac{c}{2B_R \sin\eta}, \tag{2.5}$$

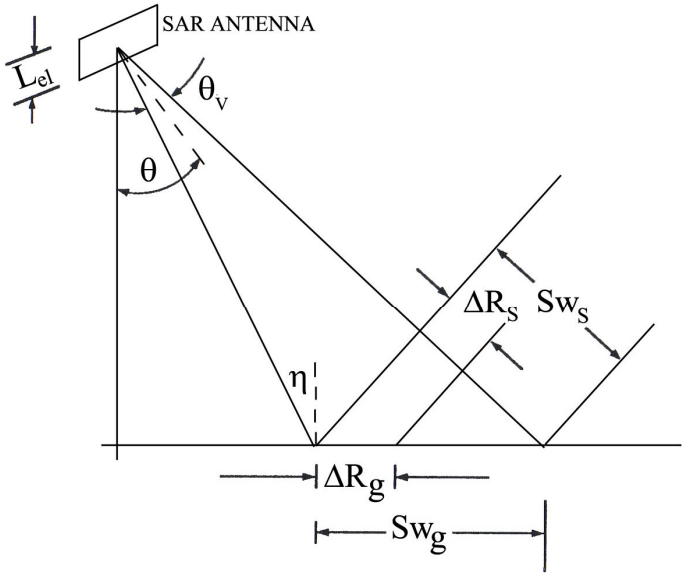

Fig. 2.4: Radar geometry illustrating the ground swath and θ_V

where B_R is the radar pulse bandwidth and η is the incidence angle. Within legal (In the government web [33] the bandwidth limits for space earth observation are detailed) and technological limitations, the range resolution can be made arbitrarily fine by increasing the pulse bandwidth at the cost of loosing sensitivity. The resolution also improves for increasing incidence angles, but this also increases the range and tends to reduce the normalized radar cross-section. The relation between slant range and ground range resolution is illustrated in Fig. 2.4.

2.3.2 Azimuth Resolution

The azimuth resolution limit of a SAR system is approximately given by

$$\delta x \geq \frac{L_{az}}{2}, \tag{2.6}$$

where L_{az} is the azimuth dimension of the antenna. This expression results from approximating the beam-width by $\theta_H = \lambda/L_{az}$. The exact expression depends on the exact beam-pattern and on how the SAR processing is implemented. Exists the possibility to improve the along-track resolution Δx it is necessary to decrease the antenna length in the along-track dimension.

2.4 The Antenna

The SAR antenna assembly typically consists of either a single high gain used for both transmit and receive consisting of a feed system or by an array of transmit/receive elements, usually organized in tiles. The key antenna parameters affecting the SAR performance are the antenna gain (or directivity) and its beam pattern. The antenna gain is directly proportional to its effective area (A_{ef}). The gain is given by the product of the

antenna efficiency and its directivity D:

$$G = \eta D = \eta \frac{4\pi A_a}{\lambda^2} = \frac{4\pi A_{ef}}{\lambda^2}. \tag{2.7}$$

The antenna efficiency is given by the product of the radiation efficiency (which depends on resistive losses) and the aperture efficiency, which depends on the illumination. Typically, to achieve the desired sensitivity for space-borne systems, aperture gains well over 30 dB or more are required.

2.4.1 Minimum antenna area (zero order ambiguity analysis)

A first lower bound on the required antenna (effective) area can be derived from a zero order analysis of range-azimuth ambiguities. For a given antenna length, which as seen in (2.6) is approximately twice the azimuth, a minimum PRF can be immediately derived. This can be done in several ways, but the simplest reasoning is that for each independent *sample* in azimuth in the output image the system must acquire, at least, one raw *sample.* Thus, a SAR system should transmit, at least, one pulse every time it advances a distance of $L_{az}/2$ and the minimum PRF is, therefore

$$PRF_{\min} = \frac{2V_s}{L_{az}}. \tag{2.8}$$

This minimum PRF sets a maximum unambiguous slant-range swath

$$\text{swath}_{\text{slant,max}} = \frac{c}{2 \cdot PRF_{\min}} = \frac{c \cdot L_{az}}{4 \cdot V_s}, \tag{2.9}$$

Which projected onto ground range gives a maximum swath of

$$\text{swath}_{\max} = \frac{c \cdot L_a}{4 \cdot V_s \sin\theta}. \tag{2.10}$$

To avoid out of swath targets to produce significant ambiguous echoes, their signal must be suppressed by the radiation pattern in elevation of the antenna. In other words, the foot-print of the antenna must be smaller than the maximum swath. Combining the expression of this footprint with (2.10) yields

$$A_{eff} \geq \frac{4 \cdot V_s \lambda \tan\theta}{c}. \tag{2.11}$$

This expression gives the minimum area of a SAR antenna given the carrier wavelength, the incidence angle, and the orbital velocity, which is set by the orbital height and almost constant for the range of useful orbital altitudes. It is noteworthy that this minimum area is independent of other requirements, such as sensitivity or resolution.

For every band we will have different minimum antenna areas, as it is shown in Fig. 2.5.

It is worth noting that this minimum antenna area results from a zero order analysis, in

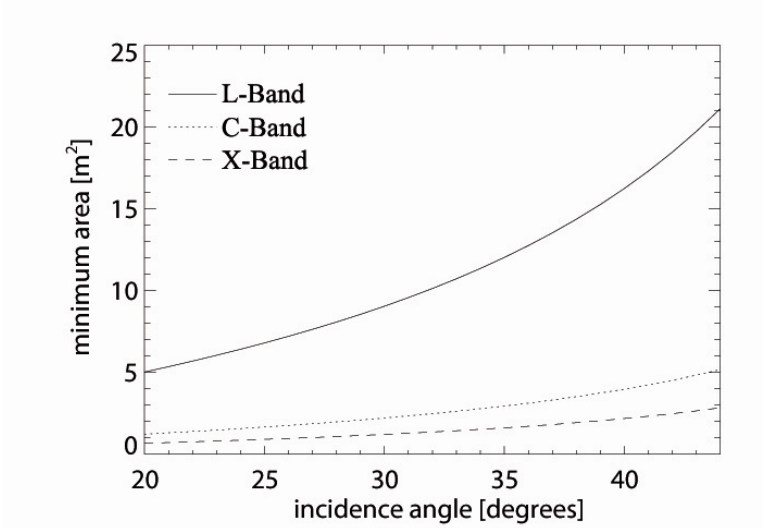

Fig. 2.5 Minimum required antenna area for LEO SAR system at different frequency bands.

which it is assumed that the PRF must satisfy the Nyquist minimum sapling rate. It is worth noting that, strictly speaking, it is possible, to some extent, to operate with sub-Nyquist PRF values by reducing the effective Doppler bandwidth, which results in a loss of azimuth resolution. However, the condition given in (2.11) is both widely assumed in the literature and satisfied by all existing SAR missions.

2.5 Ambiguity Analysis

In section 2.4.1 a zero order ambiguity analysis was presented. In this analysis it was assumed that to reject ambiguous radar echoes corresponding to out of swath target it is necessary that the swath be smaller than the footprint of the antenna pattern on the ground. However, the size of this footprint was implicitly given in terms of the one-way 3 dB beamwidth, which for a uniform antenna illumination in elevation is given by

$$\theta_{H,3dB} = \frac{\lambda}{L_H}. \tag{2.12}$$

This criterion would only provide 6dB suppression for ambiguous targets located at the edges of the footprint. Considering the large dynamic range of σ_0, it is obvious that this suppression is insufficient. The existence of range ambiguities caused by the antenna pattern elevation side-lobes is illustrated in Fig. 2.7.

Likewise, the expression for the minimum PRF given in (2.8) can be related to the need to sample the Doppler spectrum at least at the Nyquist rate (twice the Doppler bandwidth). Here the Doppler bandwidth is determined by the antenna beam-width in the azimuth direction. Expression (2.8) corresponds to the Nyquist rate considering the 6dB Doppler bandwidth, which does not prevent spectral components corresponding to the side-lobes of the antenna pattern to alias back into the main part of the spectrum, which result in azimuth ambiguities. This spectral folding is illustrated in Fig. 2.6.

For a given range and azimuth antenna pattern, the PRF must be selected such that the total ambiguity noise contribution is very small relatively to the signal. Alternatively, given a

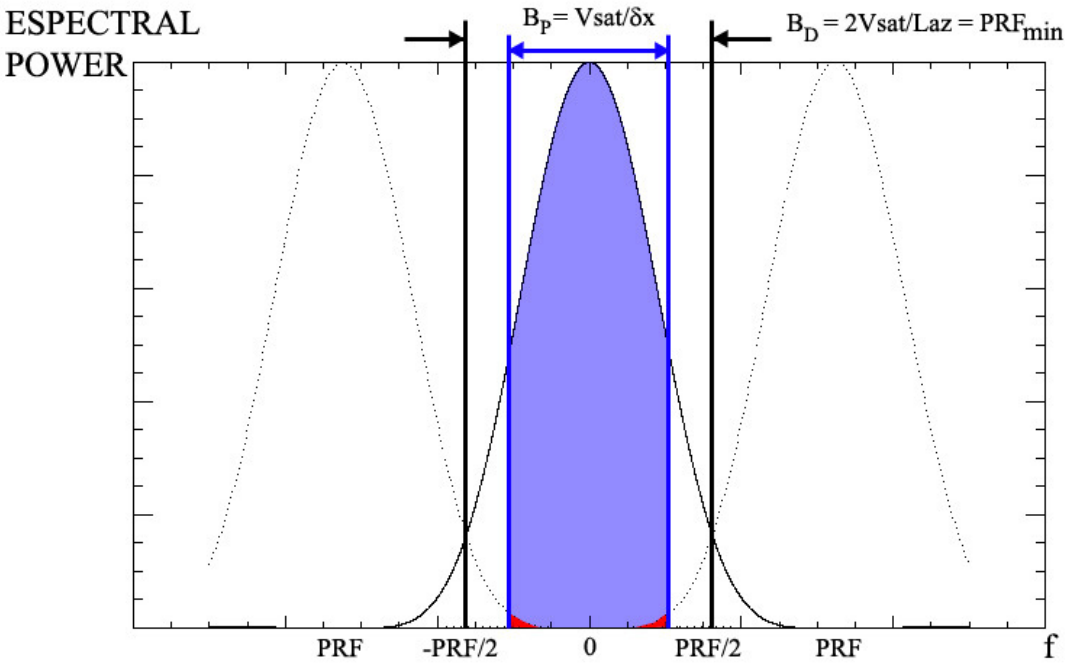

Fig. 2.6: Spectral folding of Doppler spectrum for PRF=B_D

PRF or range of PRFs, the antenna dimensions and/or weighting (to lower the sidelobe energy) must be such that the signal-to-ambiguity noise specification is met.

The ambiguous signal power at some Doppler frequency f_0 and some time delay τ_0 can be expressed as [36]

$$S_a(f_0,\tau_0) = \sum_{m,n\neq 0} G^2\left(f_0 + m\cdot\mathrm{PRF}, \tau_0 + n/\mathrm{PRF}\right)\cdot\sigma_0\left(f_0 + m\cdot\mathrm{PRF}, \tau_0 + n/\mathrm{PRF}\right), \tag{2.13}$$

where m and n are integers $G^2(f, \tau)$ is the two-way far field antenna power pattern, and σ^0 is the radar reflectivity. The integrated ambiguity to signal ratio (ASR) is therefore given by

$$ASR(\tau) = \frac{\sum_{m,n\neq 0}\int_{-B_p/2}^{B_p/2} G^2\left(f_0 + m\cdot\mathrm{PRF}, \tau_0 + n/\mathrm{PRF}\right)\cdot\sigma_0\left(f_0 + m\cdot\mathrm{PRF}, \tau_0 + n/\mathrm{PRF}\right)df}{\int_{-B_p/2}^{B_p/2} G^2\left(f_0,\tau_0\right)\cdot\sigma_0\left(f_0,\tau_0\right)df}, \tag{2.14}$$

where B_p is the processing bandwidth. This processing bandwidth is upper bounded by the PRF. However, taking a smaller value can help filter out an important part of the Doppler spectrum aliased into the main Nyquist window so it can be improved in the processor at the cost of loosing azimuth resolution.

The ASR is written as a function of τ, or equivalently the cross-track position in the image. This expression for ASR requires knowledge of the two-dimensional antenna pattern, and of the target reflectivity to be formulated in terms of the Doppler frequency and the time delay. Additionally relations are required to derive these quantities from the measured data. Typically, antenna pattern are given as a function of local incidence angle. For design

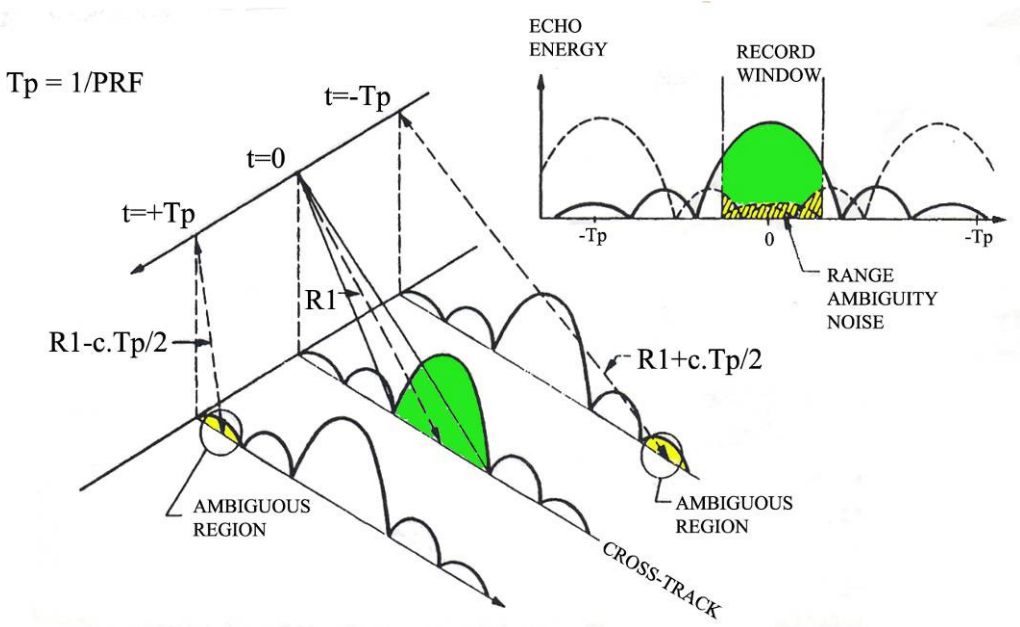

Fig. 2.7: Illustration of SAR range ambiguities

purposes it is more useful to separate the azimuth and the range components.

2.5.1 Azimuth ambiguity

The ratio of the ambiguous signal to the desired signal, within the SAR correlator azimuth processing bandwidth, is commonly referred to as the azimuth ambiguity to signal ratio (AASR). The AASR can be estimated using the following equation:

$$\mathrm{AASR} = \frac{\sum_{m\neq 0} \int_{-B_p/2}^{B_p/2} G^2\left(f + m\cdot \mathrm{PRF}\right)\cdot df}{\int_{-B_p/2}^{B_p/2} G^2\left(f\right) df}, \tag{2.15}$$

where it is assumed that target reflectivity is uniform across de scene in range and in azimuth. Also, it is assumed that the 2-D antenna pattern can be separated as the product of an elevation and an azimuth pattern, which is a reasonable approximation for the most significant side-lobes. The AASR as given by the previous equation is typically specified to be on the order of -20dB. However, even at this value ambiguous signals can be observed in images that have very bright target adjacent to dark targets.

2.5.2 Range Ambiguity

Range ambiguities result from preceding and succeeding pulse echoes arriving back at the antenna simultaneously with the desired return. This phenomenon is typically not significant for airborne SAR data, since the spread of the echo is very small relative to the interpulse period. However, for space-borne radars, where several interpulse periods (Tp=1/PRF) elapse between transmission and reception of a pulse, range ambiguities can become significant

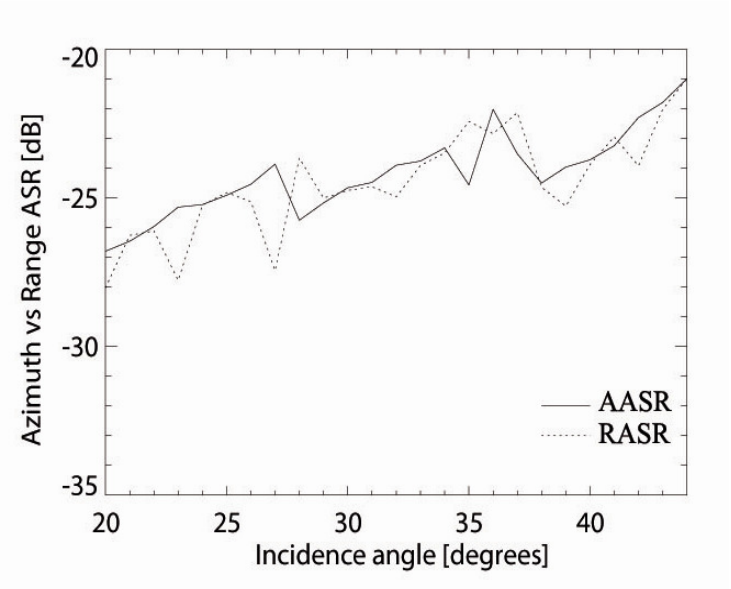

Fig. 2.8 Azimuth & Range ASR vs. Incidence Angle, the swath width 30 km and L-Band.

To derive the exact value of the range ambiguity to signal ratio (RASR), consider that, at a given time t_i within the data record window, ambiguous signals arrives from ranges of

$$R_{i,j} = \frac{c}{2}\cdot\left(t_i + \frac{j}{\mathrm{PRF}}\right), \tag{2.16}$$

where j, the number (j=0 for the desired pulse), is positive for preceding interfering pulses and negative for succeeding ones.

The integrated RASR is then determined by summing all signal components within the data window arising from preceding and succeeding pulse echoes, and taking the ratio of this sum to the integrated signal return from the desired pulse.

For any given resolution cell, the power of the ambiguous signals is proportional to

$$S_{i,a} = \sum_{j\neq 0} \frac{\sigma_{i,j} G_{i,j}^2}{R_{i,j}^3 \sin(\theta_{i,j})}, \tag{2.17}$$

where σ_{ij}^0 is the normalized backscatter coefficient at a given incidence angle, θ_{ij}, and G_{ij} is the cross-track antenna pattern at that incidence angle, while the signal of interest is given by.

$$S_i = \frac{\sigma_{i,0} G_{i,0}^2}{R_{i,0}^3 \sin(\theta_{i,0})}, \tag{2.18}$$

and, finally, the RASR is given by

$$\mathrm{RASR} = \frac{\sum_i S_i}{\sum_i S_{i,a}}, \tag{2.19}$$

the average ratio between signal of interest and ambiguous signal levels.

2.6 PRF Selection.

The set of values that the PRF can assume is constrained by a number of other factors. The preceding discussions on azimuth and range ambiguities, the AASR and RASR are both highly dependent on the selection of PRF. Its selection is further constrained for a SAR system that has a single antenna for both transmit and receive. Considering that ina a space-borne, at any given time, there are a number of pulses in the air, the transmitted pulses must be interspersed with the data reception. Additionally, the PRF must be selected such that the nadir return from succeeding pulses is excluded from the data window.

.

The transmit interference restriction on the PRF can be written as follows,

$$\begin{aligned} \mathrm{Frac}\left(2R_1.\mathrm{PRF}/c\right)/\mathrm{PRF} &> \tau_P + \tau_{RP} \\ \mathrm{Frac}\left(2R_N.\mathrm{PRF}/c\right)/\mathrm{PRF} &< 1/PRF - \tau_{RP} \\ \mathrm{Int}\left(2R_1.\mathrm{PRF}/c\right) &= \mathrm{Int}\left(2R_N.\mathrm{PRF}/c\right) \end{aligned} \tag{2.20}$$

where R_1 1is the slant range to the first data sample (i.e. j=0, i=1), R_N is the slant range to the last (Nth) data sample in the recording window, τ_P is the transmit pulse duration, and τ_{RP} is the receiver protect window extension about tp. The function Frac and Int extract the fractional and the integer portions of their arguments, respectively. These relationships are illustrated in the timing diagram, Fig. 2.10

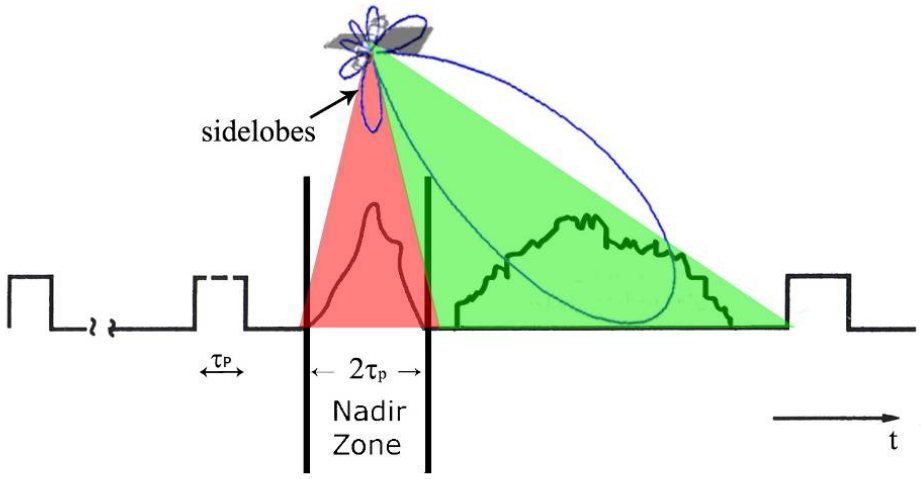

Fig. 2.9 Nadir interferences

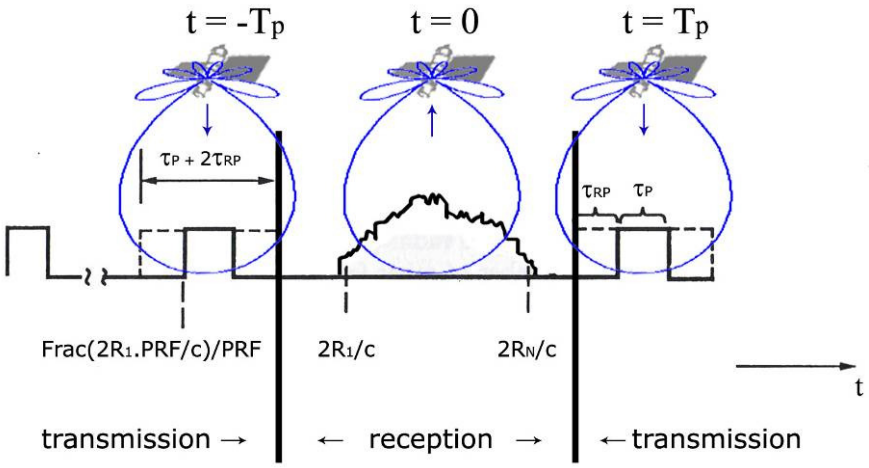

Fig. 2.10 Transmit interferences

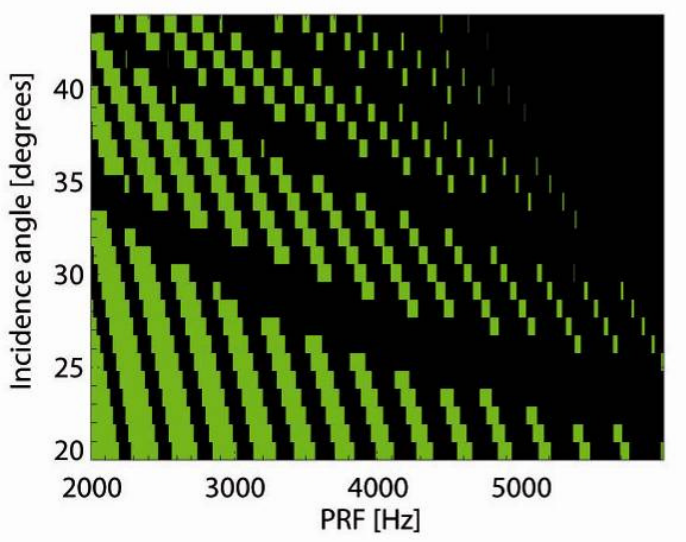

Fig. 2.11 PRF against η illustrating excluded zones as a result of transmit and nadir interference. We have considered a 30 Km swath width.

The nadir interference restriction on the PRF can be written as follows:

$$\begin{aligned} &2h/c + j/PRF > 2R_N/c \\ &2h/c + 2\tau_p + j/PRF < 2R_1/c \end{aligned} \qquad j=0,\pm1,\pm2,\ldots,\pm,n_h \qquad (2.21)$$

where $H \cong R_s - R_t$ is the sensor altitude above the surface nadir point. We have assumed in the above analysis that the duration of the nadir return is $2\tau_p$. The actual nadir return duration will depend on the characteristics of the terrain. For rough terrain the significant nadir return could be shorter or longer than $2\tau_p$. An example is given in Fig. 2.9.

Then, the range of PRFs values is established by the maximum acceptable range and azimuth ambiguity-to-signal ratios, as well as the transmit and nadir interference. At some look angles, there may be no acceptable PRFs that achieve the minimum requirements. In general, as the off-nadir angle is increased, the PRF availability is reduced and the ambiguity requirements must be lowered to find acceptable PRFs.

2.7 Signal Parameters (f_0, τ_0, polarization)

The radar transmits a waveform s(t) which is backscattered by a target at range R, so that the echo corresponding to that target arrives with a time-delay $\tau = 2R/c$. The energy of the input signal is just

$$E = P_S \tau_P, \tag{2.22}$$

where τ_p is the duration of the pulse and P_s is the average power this duration (which for chirp signals is also the peak power). Long pulses of tolerable average power can be used to obtain large energy satisfying the detectability requirements, while at the same time a wide bandwidth can be used to obtain good resolution.

2.7.1 Frequency Band

A fundamental system parameter is the center frequency of the system. Its choice depends on the applications, the required resolution, and on technological aspects. In this study we have considered three possible bands: L-band, C-band and X-band. Lower frequencies (P-band) have been excluded from the start because of the large dimensions of the required antennas. Higher frequencies have been discarded because of the intrinsic technological difficulty associated to them.

At L-band, the longer wavelengths are appropriate for missions that require a larger degree of penetration, for example for detection and imaging of soil moisture, or for retrieval of biomass. Because the available bandwidth, both from a technological and from a legal point of view, scales with frequency, this increased penetration goes at the expense of resolution.

Moving to the high frequency end, X-band (10 GHz) is the preferred option for high resolution systems. This is due the availability of large bandwidths (for example, TerraSAR-X uses up to 300 MHz bandwidth) and the technological maturity of space ready X-band components. Also, at higher frequencies the antenna area is smaller for a given antenna gain, which enables the design of more compact systems.

The C-Band (typically around 5.4 GHz) is a compromise between the two extremes, offering reasonable performance in terms of resolution and surface penetration. For the past 15 years C-Band was the preferred choice for some very well performing SAR systems like for the ESA missions ERS-1, -2 and ENVISAT due to the technological availability at the time of system definition and in order to maintain data continuity over a long period. All three missions are part of the strong Astrium GmbH SAR heritage basis, due to its role as prime contractor, mission prime and SAR subsystem supplier.

2.7.2 Bandwidth and pulse duration.

The slant-range resolution of a SAR system is given by the two-way speed of light divided by the transmitted pulse bandwidth,

$$\delta R = \frac{c}{2B_R}. \tag{2.23}$$

Using a chirp signal, the required bandwidth is achieved using a frequency modulated signal, where the frequency varies linearly over the duration (τ_p). By increasing the pulse duration (decreasing the chirp rate) higher energy pulses can be obtained with a reasonable peak power (which is a technological limitation), as expressed by (2.22).

During the time that a given target is observed by a SAR system the corresponding echoes are first received with a positive Doppler frequency shift, while the system is approaching the target, which decreases until a maximum negative Doppler shift when the target exits the radar beam. This Doppler shift distorts the received signal. In the case of a chirp signal, this distortion introduces an apparent range shift, which is more severe for lower chirp rates. This apparent shift should be small compared to the range resolution. This considering the Doppler bandwidth, this condition can be expressed as

$$\tau_p \ll \frac{L_{az}}{2V_s}, \tag{2.24}$$

where L_{az} is the length of the SAR antenna. This is well satisfied for current space systems.

2.7.3 Polarization.

SAR systems, like most radar systems, can be designed to operate either in a single polarization mode, usually transmitting and receiving in the same linear polarization, or designed to operate in a number of polarimetric modes:

1. Light polarimetry: in this mode the system transmits in a fixed polarization (which can be linear or circular) and receives in two orthogonal polarizations. For example, the system may transmit in vertical polarization and receive in both vertical and horizontal, in which case the two channels are typically identified as VV and HV. Light polarimetry is useful for some applications and does not imply any significant fundamental trade-off. It does, however, increase the technological complexity of the system and, everything else equal, it duplicates the data rate and downlink bandwidth requirements.
2. Alternating polarization: in this mode (implemented, for example, in ENVISAT), the system sends a number of pulses in one polarization, receiving in both polarizations, followed by another series of pulses in the orthogonal polarization. System considerations are the same as in the case of light polarimetry, except for the fact that the azimuth resolution is degraded by at least a factor of two.
3. Full polarimetry: in this mode the system alternates pulses in both polarizations. In contrast to the other modes, the implementation of this mode has an impact on a number of design trade-offs.

3 SAR SYSTEM TRADE-OFFS AND DESIGN FLOW

Taking into account the trade-offs between SAR parameters discussed in previous sections, we have generated an orbital SAR mission design. This design flow corresponds to a standard strip-map mode. Due to the limited scope of this study only first order optimizations have been done.

Fig. 3.1 illustrates the complex relationship between SAR system parameters. This chart can be unravelled in a number of ways leading to different design flows depending on the starting point. In this study two possibilities have been considered:

1. An ideal case in which the entry point are a number of fundamental parameters (polarization, frequency, etc) and the desired sensitivity and range and azimuth resolutions.
2. A constraint case in which the dimensions of the antenna and the available average power are set. This procedure is useful to check the process against existing missions. It also reflects more realistically the constraints present in the planning of any real mission.

3.1 Ideal case

The design flow for the ideal case is shown in Fig. *3.2*. The range resolution (δR_g) translates directly to a required pulse bandwidth, B_R, using (2.5). Likewise, by virtue of

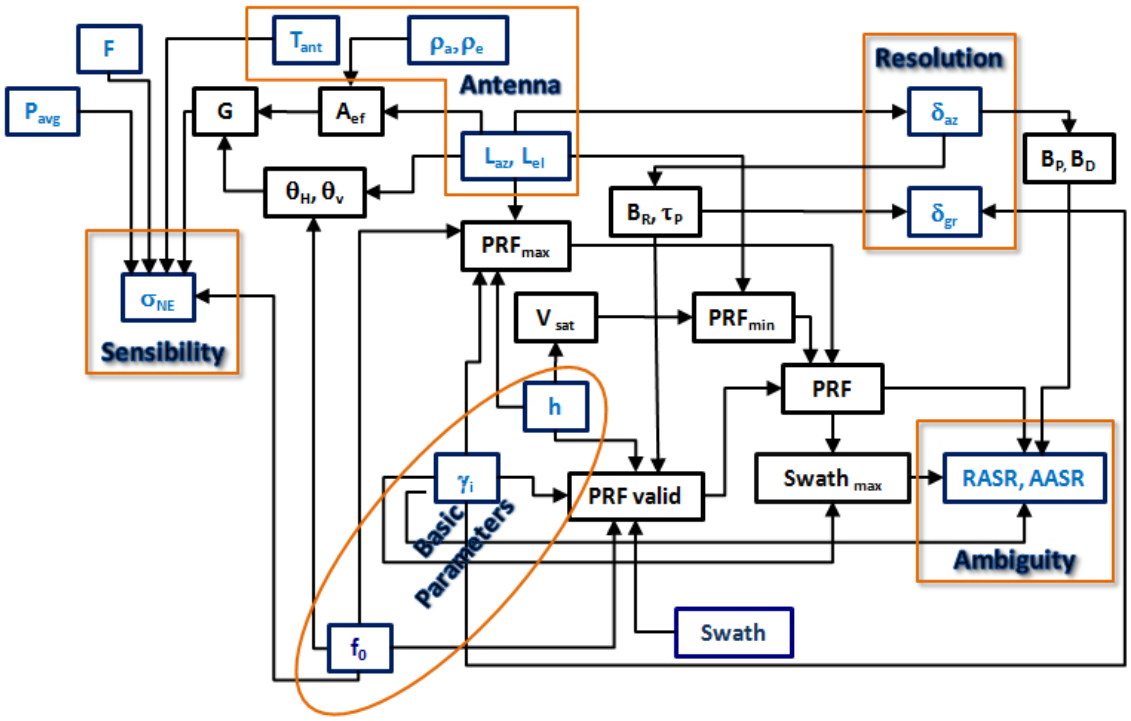

Fig. 3.1 Relationship between parameters

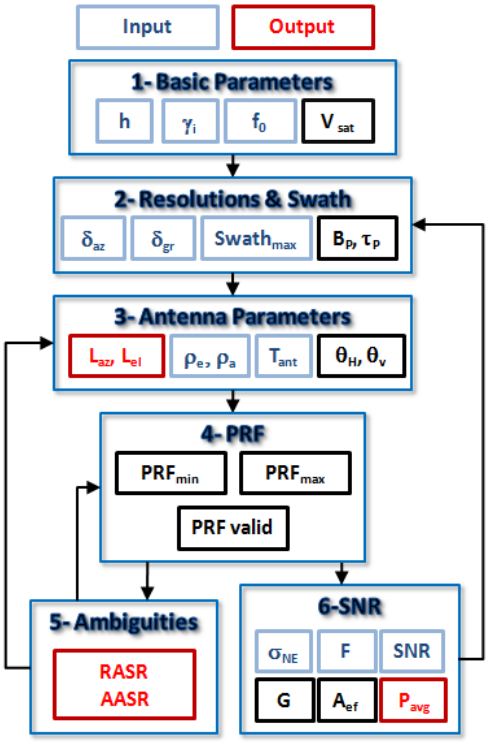

Fig. 3.2 SAR sensor design flow with fixed resolutions

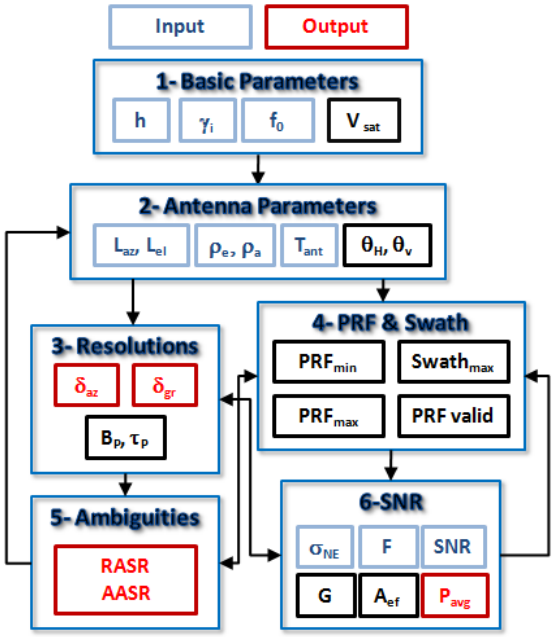

Fig. 3.3 SAR sensor design flow limited by antenna size

expression (2.6), the required azimuth resolution (δx) also translates to an antenna length (L_{az}). The minimum antenna width is determined by the minimum antenna effective area (A_{eff}). However, this minimum dimension usually results in range ambiguities above the requirements. Therefore, the design process requires an iterative process during which the antenna width and its illumination are optimized.

Once the azimuth dimension of the antenna is set, the maximum pulse duration, (2.24), and the minimum required PRF, (2.8), can be determined. The next step is the definition of a map of valid PRF values. This is done by applying the nadir interference constraint, (2.21), and the transmit interference restrictions, (2.20).

At this point it is possible to calculate AASR and RASR and to choose the valid PRF value that optimizes the ASR for every incidence angle. Fig. 2.8 shows an example of the optimal $ASR_{opt.}$ vs. the incidence angle,. η. If the optimized ASR does not satisfy the requirements, the antenna width is increased and the process is repeated.

After the antenna parameters and system bandwidth have been set, the final stage of the design is to determine the transmit power necessary to satisfy the sensitivity requirement.

3.2 Constraint case

In the constraint, Fig. 3.3 , case the starting point of the design flow are the (maximum) length of the antenna and the available average transmit power. The antenna size translates directly to an azimuth resolution (δx). Just like in the previous design, the maximum pulse

duration (2.24), the minimum PRF allowed (2.8), the maximum swath reachable (2.10) and the valid PRF values are determined.

To obtain the required AASR and RASR, the antenna width and optimum values are iteratively adjusted. The difference is that the antenna is not optimized for the ASR level, because initially it can be wider than it needs to be. On the other hand, with wider antenna values we can relax more the PRF conditions if the ASR level is far from -20dB.

The final stage is calculating the transmit power required to get the range resolution for a specified sensitivity. For a fixed transmit power, a higher sensitivity can be attained by decreasing the signal bandwidth at the cost of range resolution (2.5). More resolution required proportionally more power.

3.3 Design Flow Validation: TerraSAR-X "revisited"

Trying to validate our design methodology we have tested the design flows considered in this chapter. In order to validate the process, first main parameters of the TerraSAR-X mission have been set as constraints in order to try to reproduce its final specifications. This exercise is also useful to evaluate how tight the design of TerraSAR-X is.

The objective is to obtain a similar system as the actual TerraSAR-X, starting from its mission parameters, which are listed in Table 3.1.

The minimum antenna area has been calculated using (2.11) and represented, as a function of the incidence angle in *Fig. 3.4*. This yields a minimum area of 0.69 m^2 for a 20º incidence angle and 2.95 m^2 for a 45º incidence angle. This latest figure would, therefore, set the lower bound for the antenna area, without taking into account the ambiguity requirements.

TerraSAR-X nominal strip-map azimuth resolution is 3 m, for which the optimal antenna length is about 6 m. TerraSAR-X actual antenna length is around 4,8 m, which implies that, the azimuth resolution have been relaxed in order to meet ASR requirements. For this reason, a significant fraction of the Doppler Bandwidth is being filtered-out. this length and the previously obtained minimum area, the minimum antenna width is 0.5 m.

Following the design flow, the valid PRF values are calculated and illustrated in *Fig. 3.5*. Then, for each incidence angle the design procedure checks if there is a valid PRF that gives the desired ASR for the desired 30 Km swath. If this condition is not achieved the antenna width is and the process is repeated. In this particular case, the ASR requirements are met for the entire range of incidence angles for an antenna width of 0.7 m..The ASR values finally obtained are illustrated in Fig. 3.6. As specified, all values are less than 20 dB.

f_0	9.65 GHz (X-Band)
Orbital altitude	514 Km.
Incidence angle	between 20º and 45º
Resolutions	δR_g= 1'7m δx= 3 m
Swath	30 Km
σ_0	-20 dB
ASR	20 dB
Mode	Strip-map
Polarization	single

Table 3.1 TerraSAR-X mission parameters

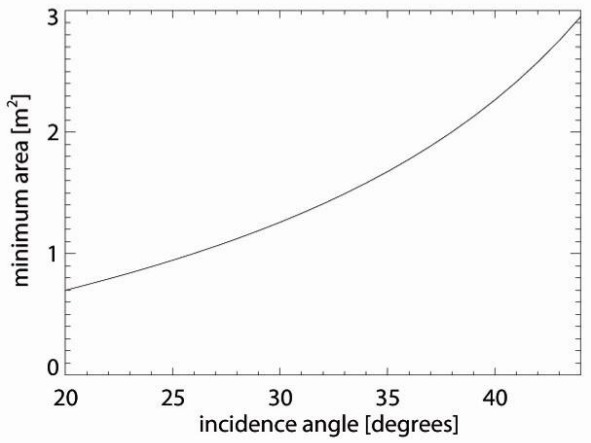

Fig. 3.4 TerraSAR-X: Minimum antenna area

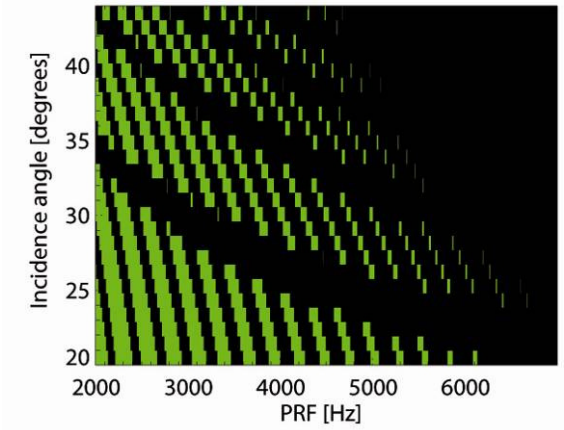

Fig. 3.5 TerraSAR-X: non interference PRF values

In order to calculate the AASR it has been assumed that the illumination of the antenna, like in most orbital missions, is uniform in azimuth. In practice it found that an azimuth tapering does not improve the AASR levels while reducing the antenna gain. In range however, the RASR depends significantly on the tapering in elevation of the antenna. This tapering is optimized, in terms of SNR and ASR for each operating mode of the system. In our model this optimization has been limited to choosing between no tapering, which works best for large incidence angles, and a Hanning tapering, which works best for small incidence angles (see Fig. 3.7).

Incidence dependent tapering requires a relatively complex active antenna, like that of ENVISAT's ASAR and TerraSAR-X, which is also required for electronic steering in elevation (in contrast to mechanical steering accomplished by rotating the platform). It is, therefore, unclear that it is a viable solution for a compact, low-cost, mission.

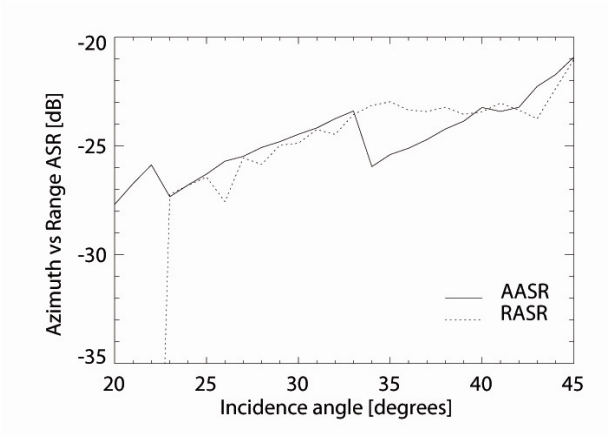

Fig. 3.6 TerraSAR-X: AASR and RASR with antenna adjusted to optimum

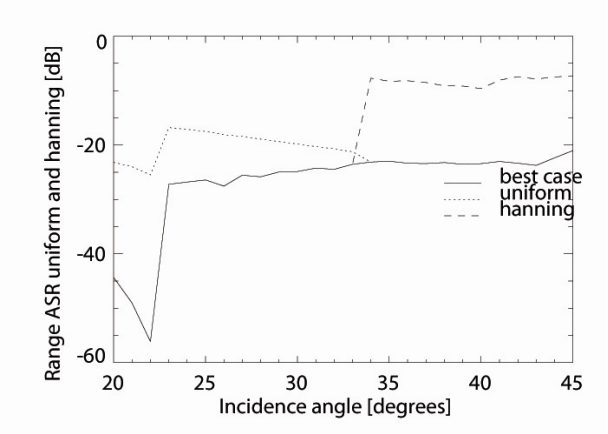

Fig. 3.7 TerraSAR-X: uniform and hanning tapering in elevation

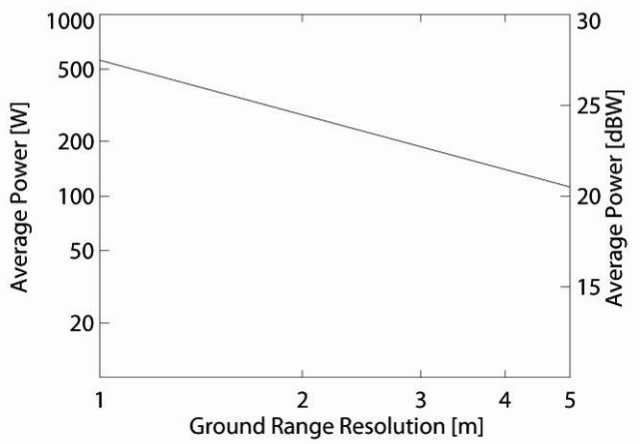

Fig. 3.8 TerraSAR-X: Average Power vs. Range Resolution

Parameters	TerraSAR	"TerraSAR revisited"
Antenna Length	4,784 m	4,8 m
Antenna Width	0,704 m	0,7 m
Average Transmit Power	360 W	300 W

Table 3.2 TerraSAR design comparison

The final step is determining the required average transmit power. Fig. 3.8 shows the required power as a function of the desired range resolution necessary to achieve -20 dB of Noise Equivalent σ_0. For 1'7 m range resolution the required transmit power is around 300W.

Table 3.2 shows a comparison of the main mission parameters obtained and their TerraSAR-X counterparts. It can be concluded that even though the design procedure us limited to first order optimizations, it yields valid and realistic results.

4 S3D BETA VERSION (SOFTWARE FOR SAR SENSOR DESIGN)

The S3D can be divided in 2 parts. The front-end is the interface that allows the user to introduce the parameters and see the results. The back-end is made up by a list of routines that are called by the front-end.

4.1 IDL Introduction

The language used in the implementation of the S3D is IDL (Interactive Data Language).

IDL is a complete data analysis and visualization environment that is used in a wide range of science and engineering disciplines for processing and analyzing numerical and image data. It is often used in advanced science/technical courses. IDL integrates an array-oriented language with numerous mathematical analysis and graphical display techniques, thus giving you more flexibility than other mathematical languages.

4.2 S3D Back-end description

A list of routines and functions, 64 has been programmed in order to turn the mathematical equations described in chapter 2 into processes that allow us to design the sensor.

In order to understand the capabilities of the software, a brief description of the most relevant routine follows.

- ***mysar:*** Creates a structure with the parameters of the SAR mission.
- ***orbit_vel***: Calculates the satellite velocity as shown in equation (2.1)
- ***areamin:*** Based on the theory explained in chapter 2.4.1, it calculates the lower bound on the required antenna (effective) area from a zero order analysis of range-azimuth ambiguities. It establishes the starting point of the antenna. The plotted result is shown on Fig. 4.2.
- ***PRFbad:*** Based on the theory explained in chapter 2.6, it calculates the PRF valid values. Optionally, it visualizes these valid PRF values for a range of incidence angles, as seen in Fig. 4.3
- ***sarsens:*** Using Radar equation (chapter 2.2) it is easy to find a relation between the Average Power and the Range Resolution. The use of the plot, Fig. 4.5, could be very useful in the constraint case in which the range resolution could be adjusted to establish a reasonable Average Power.
- ***saramb:*** This function calculates the Range and Azimuth ambiguities as explained in section 2.5. The values of ASR are given for one concrete incidence angle, PRF, antenna size and illumination tapering.

- ***bestPRF:*** This function iterates saramb in order to find the PRF value that achieves the best ASR rejection for every incidence angle. The ASR results can be plotted as showed in Fig. 4.4
- ***bestLel:*** Starting from the minimum antenna width, it iterates bestPRF in order to find the minimum width that satisfies the ASR requirements for every incidence angle.

4.3 S3D Front-end description

The S3D front-end consists in 3 graphic user interfaces (GUI) based on the 2 design flow cases described in chapter 3. The first one is only to choose the mission design flow, Fig. 4.1. The Ideal Case GUI, Fig. 4.6, shows the steps to follow in case the mission has resolution requirements and freedom antenna size. Finally, the Constraint Case GUI, Fig. 4.7, follows the design flow in which the mission has to be built from an antenna specific size. Every button of the GUI executes an IDL routine from the required action. Input and output parameters for ideal and constraint case are listed.

- Ideal Case. Input parameters: SAR Mission Version, Sigma Noise, Ambiguity Signal Ratio, Satellite altitude, Incidence Angle Range, Frequency, Pulse Time, Azimuth Resolution, Range Resolution, Swath, PRF Range and Aperture Efficiency.
- Ideal Case. Output parameters: PRF Valid values, Antenna Length, Antenna Width, Average Power Required, ASR values.
- Constraint Case. Input parameters: SAR Mission Version, Sigma Noise, Ambiguity Signal Ratio, Satellite altitude, Incidence Angle Range, Frequency, Pulse Time, Antenna Length, Antenna Width, Aperture Efficiency, Range Resolution, Swath and PRF Range.
- Constraint Case. Output parameters: PRF Valid values, Azimuth Resolution, Average Power Required, ASR values.

In order to reduce the process time, improvements in the implementation of the algorithms can be done. This is a preliminary version and more features can be added.

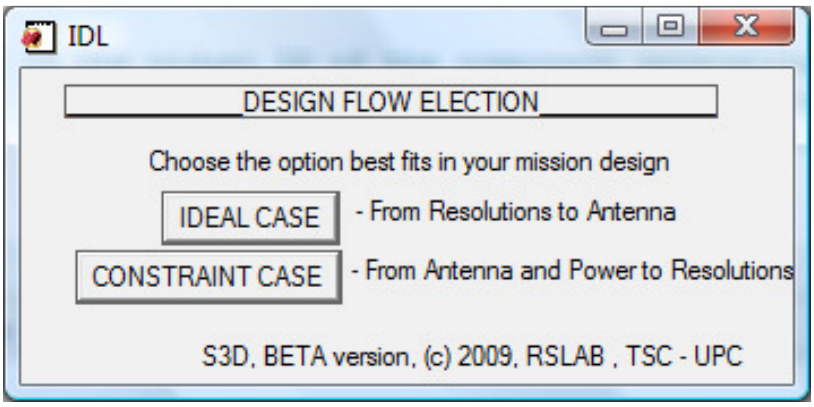

Fig. 4.1 Design Flow Selection GUI

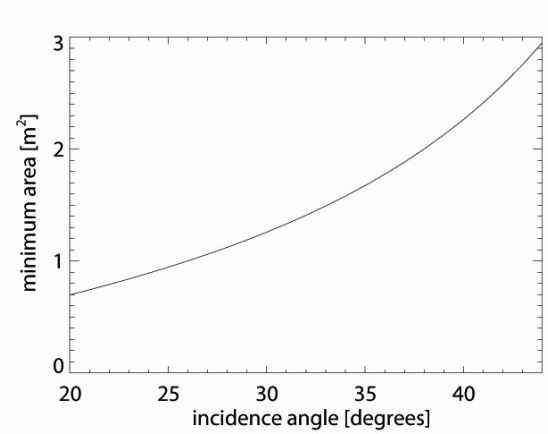

Fig. 4.2 Plotted Minimum Area vs. incidence angle from SAR mission design Software

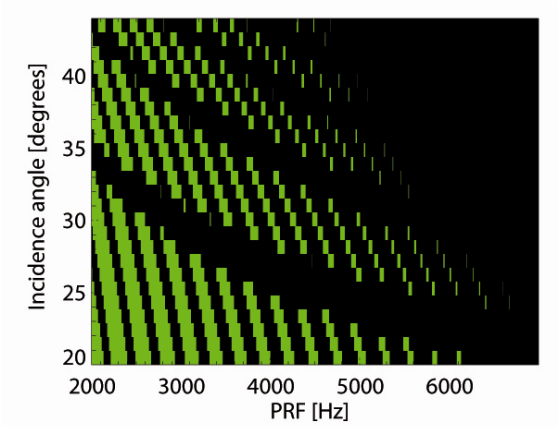

Fig. 4.3 Plotted PRF Valid Values from SAR mission design software

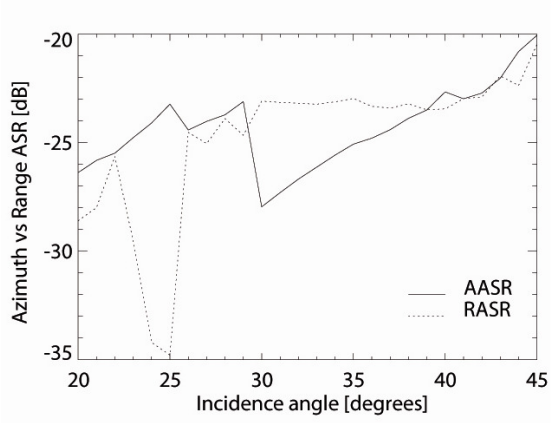

Fig. 4.4 Plotted ASR vs. incidence angle from SAR mission design software

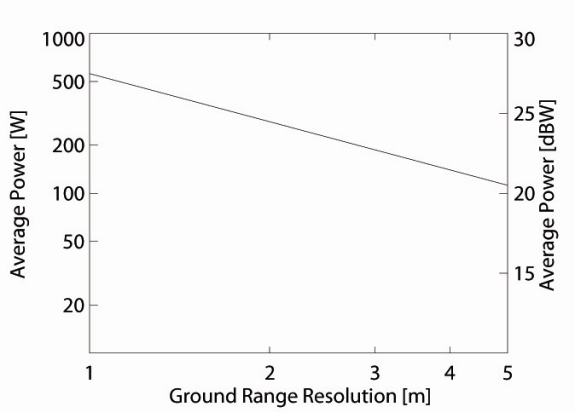

Fig. 4.5 Plotted Average Power Required vs. Range Resolution from SAR mission design software

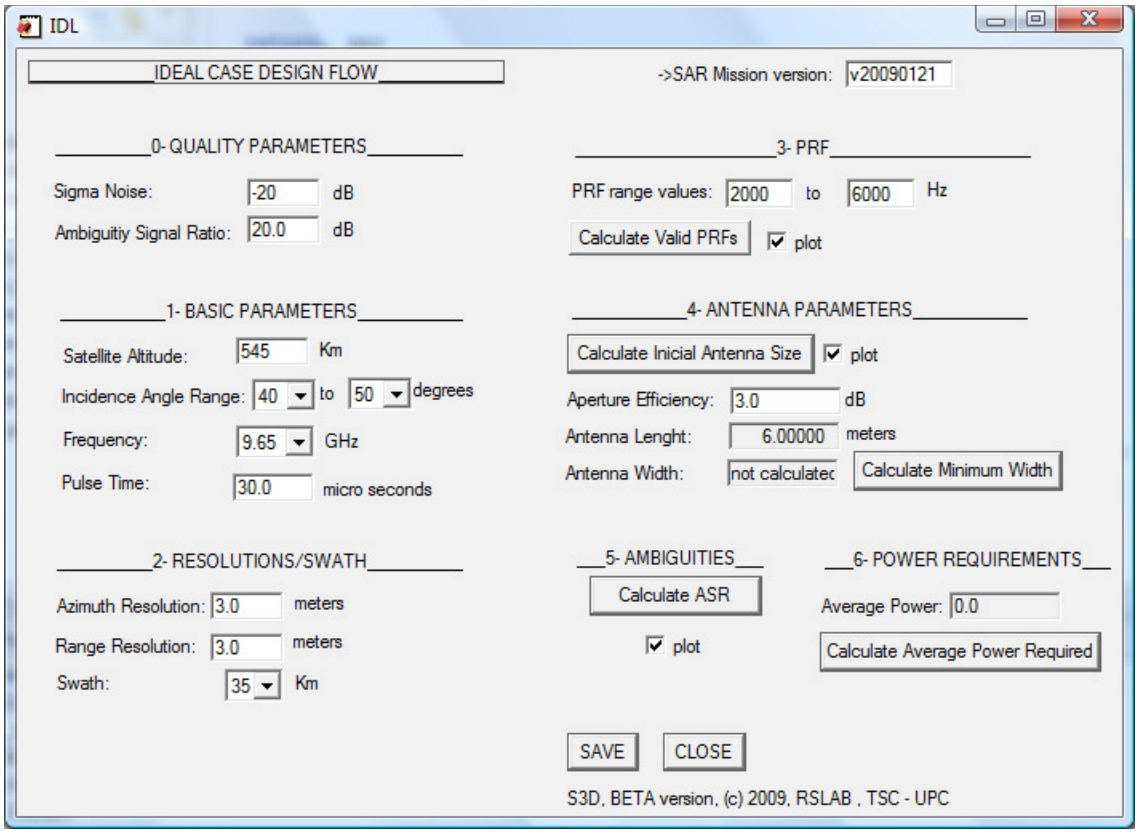

Fig. 4.6 Ideal Case Design Flow GUI of S3D

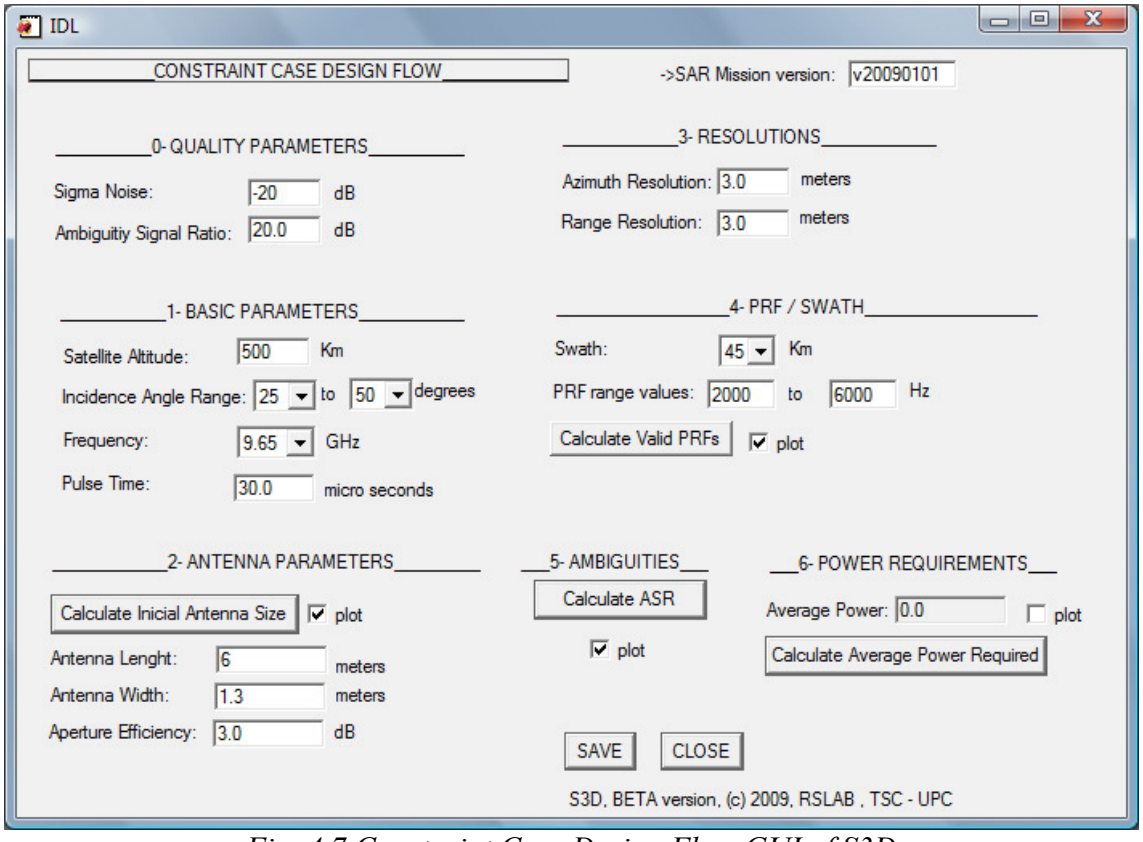

Fig. 4.7 Constraint Case Design Flow GUI of S3D

5 COMPACT MISSION DESIGN PROPOSAL

In this chapter the theory and procedures discussed in the previous chapters is applied to the design a compact SAR mission. In order to set a context for the mission, operational SAR applications are explained. Then a proposal of a possible SAR sensor is presented.

5.1 Applications of interest

This chapter contains a review of the main applications of the SAR technology. It is worth mentioning that the level of maturity of the applications presented in this chapter must be understood in the framework of the existing SAR systems.

For instance, most of the applications have been tested and analyzed at C-band, as data were available from the ERS-1/2 and the ASAR-ENVISAT missions. The validity of these applications at other bands, as for instance X-band, will be determined in the future thanks to the recent launch of the TerraSAR system.

5.1.1 Agriculture

L or C band are the recommended bands in which a SAR system has to be focused on. Nevertheless, an X-band system could be also exploited for this type of applications, especially when the quantitative retrieval of plant parameters is the objective. L- or C-band systems perform well when classification is the main issue [37].

Agriculture applications are feasible and clearly promising if polarimetric data are available. The physical reason behind this statement is that polarimetry makes data sensitive to the internal structure of the plant. This sensitivity cannot be achieved with non polarimetric SAR data. Other sources of diversity as multitime or multifrequency improve the retrieval of information.

High spatial resolution data are desirable as they make possible precision farming (Fig. 5.1), in order to retrieve internal information and inhomogeneities of single agricultural fields.

One of the most appealing features of remote sensing for the final precision farming users is the possibility to monitor the crops in time, that is, to perform multi-time acquisitions. In general weekly information could fulfill the needs of the final users.

5.1.2 Forestry

Forests are a very important part of the Earth cover and its study, in terms of National Forest Inventories, is important for both national and commercial agents [38]. The complexity of the forest cover compromises, in part, the possibility to perform an accurate

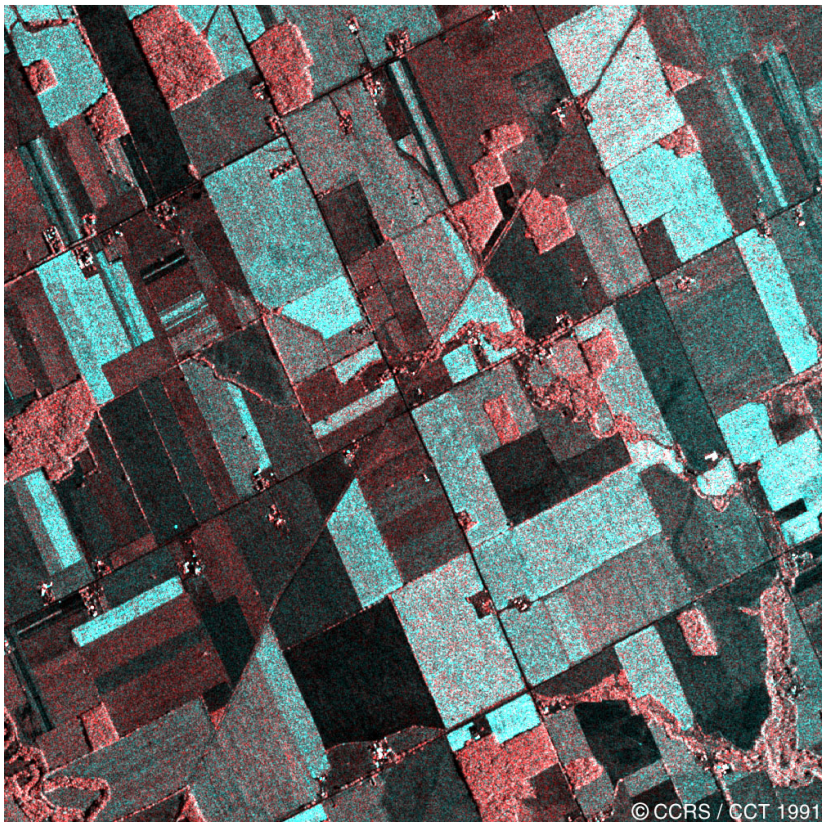

Fig. 5.1This decimated subarea of a C band SAR composite image was created from HH and HV data, colected October 18, 1991

study of forest with a single system or a single technique.

Optical systems have been employed for forest studies, but optical data are only sensitive to the upper part of the canopy, as optical waves do not penetrate. Additionally, Hyperspectral systems have been employed to study the chemistry of forest. Microwave systems, and especially SAR systems, are better suited for forestry applications since microwaves penetrate the tree canopy, allowing SAR data to be more sensitive to the geometrical structure of the tree and also to the ground.

The use of SAR data for forestry applications imposes two main constraints in the SAR system. The first is the working frequency. In order to be sensitive to the internal structure of the tree, low frequencies must be considered to assure penetration into the canopy. Most of the studies agree that the best frequency lies in the range between P- and L-band. The second constraint establishes that in order to perform an accurate study of the complexity of the forest, multidimensional SAR systems are required. In this sense, PolSAR systems have demonstrated the suitability to perform such studies.

5.1.3 Urban Monitoring

The study of urban environments with SAR systems does not impose very restrictive values for the systems parameters [38]. Perhaps, the most critical one is the spatial resolution. Nevertheless, spatial resolution may be compensated by acquiring different SAR images of the same scene under some type of diversity: time, frequency, imaging geometry, polarimetry, etc…

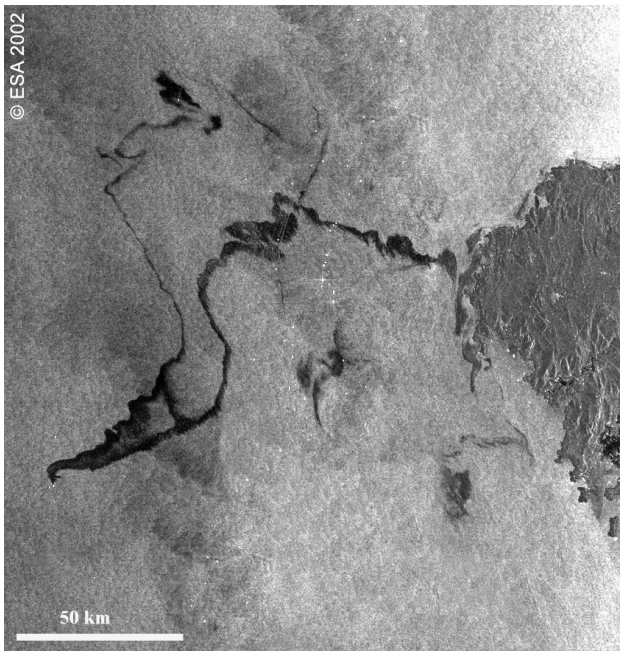

Fig. 5.2 *Envisat image of the Prestige disaster (2002). In black the oil slick released by the tanker*

Urban environments are characterized by their geometric nature. In order to be sensitive to this geometry, a SAR system must be embodied with interferometric and polarimetric capabilities. Consequently, it is possible to extract from data this geometric information making possible, for instance, 3D urban structure extraction. If the SAR system does not have these imaging modes, applications based on classification or segmentation are still possible.

Traffic monitoring is a particular application of radar that imposes important restrictions on the SAR system itself. The first of these is that in order to be sensitive to the vehicles motion, especially in the across-track direction, the system must operate in an along-track interferometric mode. From a technological perspective, this means to have two antennas in the flight direction, or to have only one but two independent receiving channels. Another important limitation is that these systems must be characterized by a very high spatial resolution, below 3 m, in order to be able to detect the vehicles. Even with a high spatial resolution not all the vehicles may be detected on the data or images as they may present a low radar cross section depending on their relative position respect to the system.

5.1.4 Coastal and Marine Applications

Most of the coastal and ocean applications are mature, such as oil-spill monitoring (Fig. 5.2), vessel detection, high-resolution wind fields (Fig. 5.3), coastal directional wave fields, shallow-water bathymetry. After a long period of research it is now time to use SAR technology as an operational system [39].

Most of the SAR applications have been motivated by the end-users themselves: coast guards, meteorological centers, ship routing, military organizations. Now, it is crucial to demonstrate that SAR coastal and ocean applications products really contribute to supporting ends users and helping them improve their activity. Therefore it is necessary now develop operational real-time products.

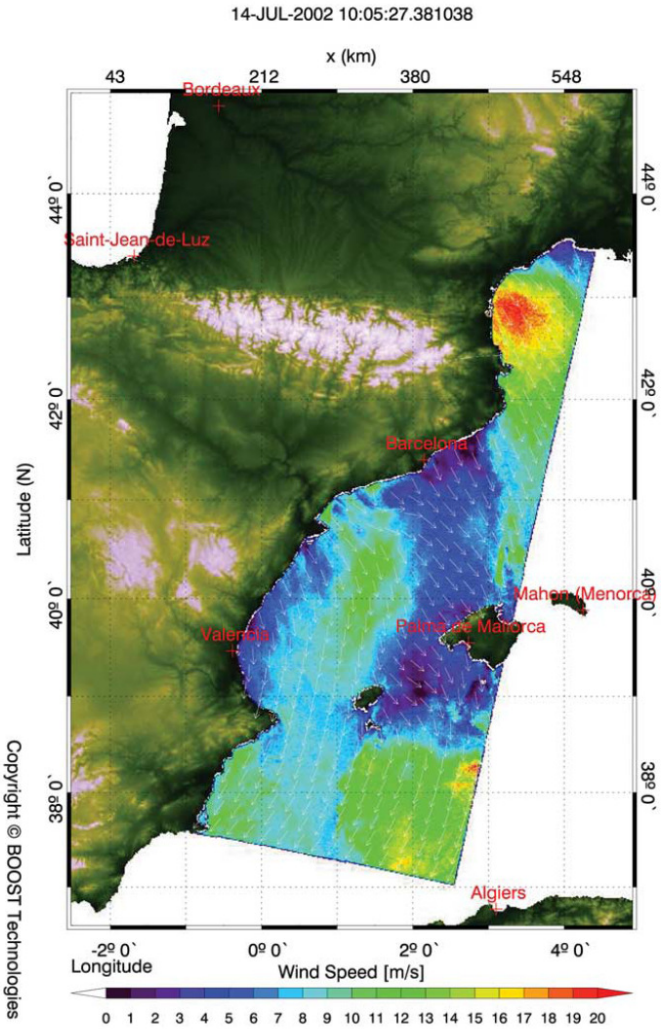

Fig. 5.3 *Example of SAR-derived 1 km resolution wind filed retrieved from Envisat (2002). From the image can be observed the relief-shadowing effect NE of Barcelona, wind acceleration at the valley output between Barcelona and Valencia and the Tramontane wind in the Gulf of Lion.*

5.1.5 The Hydrologic Cycle

There exist two main types of applications when considering snow cover monitoring and characterization. On the one hand, those applications trying to determine the snow cover area and on the other hand, a quantitative estimation of the snow cover properties [40][41]. The first one may be considered pre-operational at C-band and for incidence angles larger than 35 degrees I order to be sensitive to the snow cover. L-band data may be useful when the interest is on the sub-surface properties as scattering is little affected by the snow cover itself.

The isolated use of SAR data to monitor and to control the snow cover, especially in mountainous regions, needs still further development. Nevertheless, the information provided by these data is clearly complementary to other sources of information and some help to calibrate and to improve already existing methods to monitor the snow cover.

5.1.6 Cartography

The most important application of SAR technology nowadays is the possibility to obtain 3D topographic maps by means of SAR interferometry (InSAR). This technique is based on the fact that it is possible to derive topographic information by considering two SAR acquisitions acquired from slightly different spatial locations. The separation between both acquisitions is normally referred as baseline. In addition, the two SAR acquisitions may be obtained at the same time, i.e. single-pass InSAR, or at different times, i.e. repeat-pass InSAR [42].

The imaging mode of the SAR system, such as strip-map, ScanSAR, and spotlight, play a special role as they determine the trade-offs between spatial resolution and coverage. Although high resolution is an obvious requirement, wide swath systems also have their advantages: given a satellite SAR that is required to image every point of the Earth, a wider swath width allows for a shorter revisit cycle. This in turn increases scene coherence and is favourable for repeat-pass InSAR.

Interferometric SARs boarded in space-borne systems is the possibility to perform global mapping of topography and long-term monitoring of dynamic processes. Satellite data are at least one order of magnitude cheaper than airborne data. This is particularly true for inaccessible areas of the Earth. Space-borne remote sensing SAR sensors orbit the Earth at an altitude of typically 200 km (space shuttle) to 800 km (satellites) at inclinations ranging from 57° to 108°. Their spatial resolution is usually in the order of 5 m in azimuth and 25 m in ground range allowing for moderate averaging in azimuth for phase noise reduction to end up with square resolution elements of 25 m^2. Nevertheless, the new mission operating at X-band, as for instance the future TanDEM-X mission, allow to improve the spatial resolutions up to those obtained with airborne systems The imaged swath is about 50–100 km wide in standard imaging mode and up to 500 km with ScanSAR systems.

5.2 Orbital determination.

Satellites that monitor the global environment, like remote sensing and certain weather satellites need to scan the entire surface regularly. We have to understand satellites as a global tool and, therefore, design accordingly the most appropriate mission.

The mission's orbital design should be performed adjusting the following 6 parameters:

1. The inclination of the orbital plane.
2. The longitude of the ascending nodal line.
3. The perigee angle obtained from the ascending node.
4. The semi-major axis of the ellipse.
5. The eccentricity of the orbit.
6. The pass time at the perigee (reference initial time).

The most usual orbit for earth-mapping, earth observation, and reconnaissance satellites, as well as for some weather satellites, is a polar, or near-polar, orbit. The ground track of a polar orbiting satellite is displaced to the west after each orbital period, due to the rotation of the Earth. This displacement of longitude is a function of the orbital period (often less than 2 hours for low altitude orbits). Depending on the ground swath of the satellite, it is

possible to adjust the period (by varying the altitude), and thus the longitudinal displacement, in such a way as to ensure the observation of any point on the Earth within a certain time period.

It is common for polar orbiting satellites to choose a sun-synchronous orbit, each successive orbital pass occurs at the same local time of day. They can be particularly important for applications, where the most important thing to see may well be changes over time, which you do not want to see aliased onto changes in local time. This is an important factor for monitoring changes between images or for mosaicking adjacent images together, as they do not have to be corrected for different illumination conditions. To keep the same local time on a given pass, it is desirable for the orbit to be as short as possible, which is to say as low as possible.

In order to earth/sun-synchronize the satellite, the orbit altitude has been increased around 11 km from de 500 km assumed in Fig. 2.3. The inclination of the orbital plane must be 97'41º. An example of the track described for the satellite while crossing Catalonia is shown inFig. 5.4.

The disadvantage to polar orbit is that no one spot on the Earth's surface can be sensed continuously. It is not suitable for applications in which a little (hours or one day) revisit time is needed. To achieve a polar orbit requires more energy, thus more propellant, than does an orbit of low inclination. It cannot take advantage of the "free ride" provided by the Earth's rotation, and thus the launch vehicle must provide all of the energy for attaining orbital speed.

From the list of applications described in chapter 5.1 we can implement the ones that do not required little revisit time. Enhancing terrain features for cartography, detecting small surface movements, improving the agriculture procedures by giving information of influent parameters for the harvest…

The orbital parameters described have been summarized in Table 5.1

Nominal orbit height at the equator	511,449 km
Orbits per day	15 + 1/5
Repeat cycle	5 days
Inclination	97,41 º

Table 5.1 Orbital Parameters

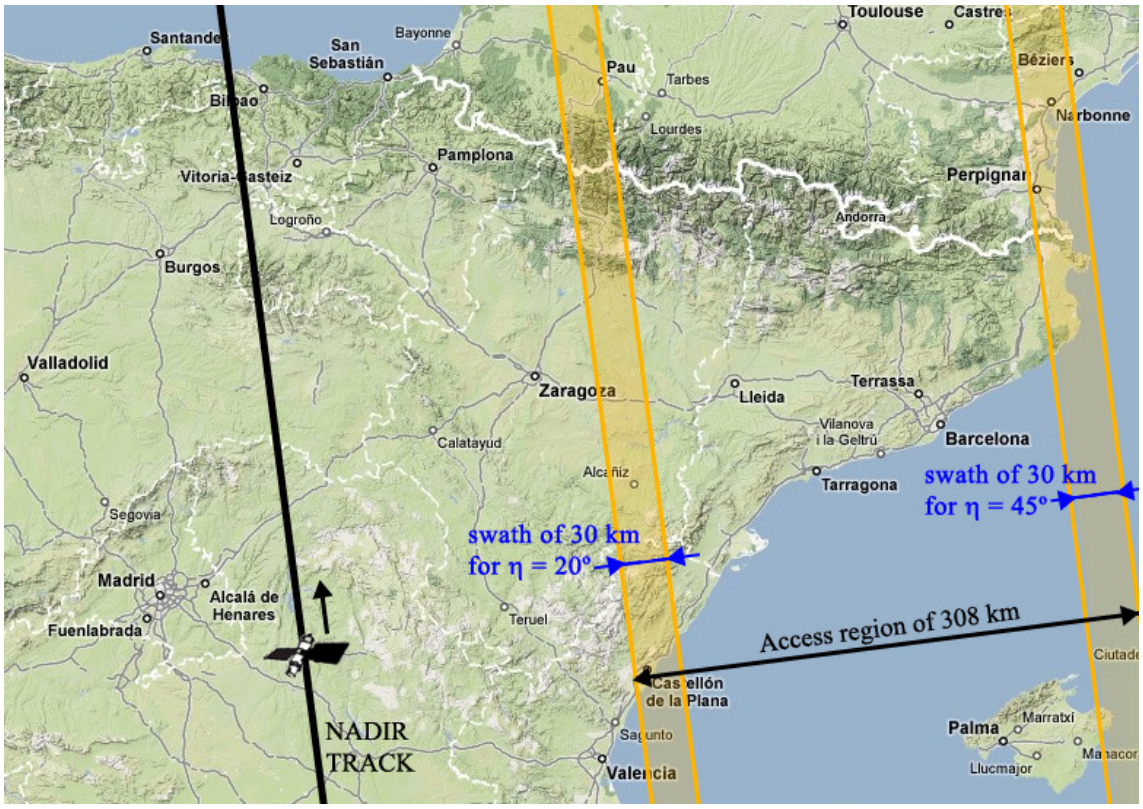

Fig. 5.4 Access region across Catalunya

5.3 Small SAR sensor proposal at L, C and X band

In order to design a SAR sensor, the design flow will be used through the software programmed. At this point, different frequency bands have been considered and the best sensor configuration has been designed for every band.

Table 5.2 shows a summary of the mission and quality requirements. ASR and σ_{NE} values have been chosen as lower bounds of the sensor quality. These ones are typical values from present SAR missions as Envisat, TerraSAR or RadarSAT. Lower values of ASR could represent too many ambiguity problems. Decreasing the final range resolution could be possible in order to improve the sensitivity in case of more was required.

As a design objective, our SAR antenna size should be the minimum required achieving a swath wide enough to the specified application. For this reason, an antenna length starting point of 5 m has been chosen and if quality requirements are not achieved it may be increased.

Booth 30 and 40 km of swath have been considered because smaller swaths are useless for certain application and bigger ones could not be achieved in the context of a small SAR because a bigger antenna should be implemented. In order to simplify the analysis only single polarization has been considered.

Analyzing the minimum area required, illustrated by Fig. 5.5, it is obvious that lower frequency bands require larger antenna sizes.

Quality Requirements	
ASR_{min}	≈ 20dB
σ_{NE}	≈ -20 dB
Ground Swath Width	30 and 40 km (both possibilities)
Mission Requirements	
Frequency bands	9,65 GHz (X-Band) 5,3 GHz (C-Band) 1,3 GHz (L-Band)
Altitude	511 Km
Incidence angle	20 to 45º
polarization	single
Laz	≤ 5 m (if quality requirements are not achieved it may be increased)

Table 5.2 Quality and Mission Requirements

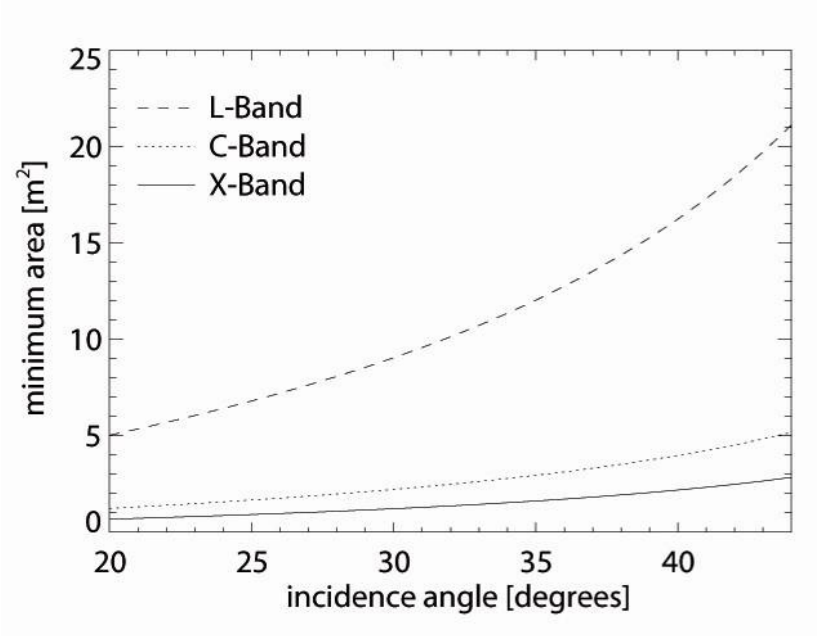

Fig. 5.5 L, C and X band initial antenna areas

The azimuth resolution values are antenna length dependent. Lower bands need bigger antennas at the cost of losing resolution. However, each band has different capability of penetration and the final SAR application will tell us the appropriated bands to be used.

Within legal and technological limitations, the range resolution can be made arbitrarily fine by increasing the pulse bandwidth at the cost of losing sensitivity.

Looking at the PRF, for larger swath less valid PRF values are left. The resulting valid

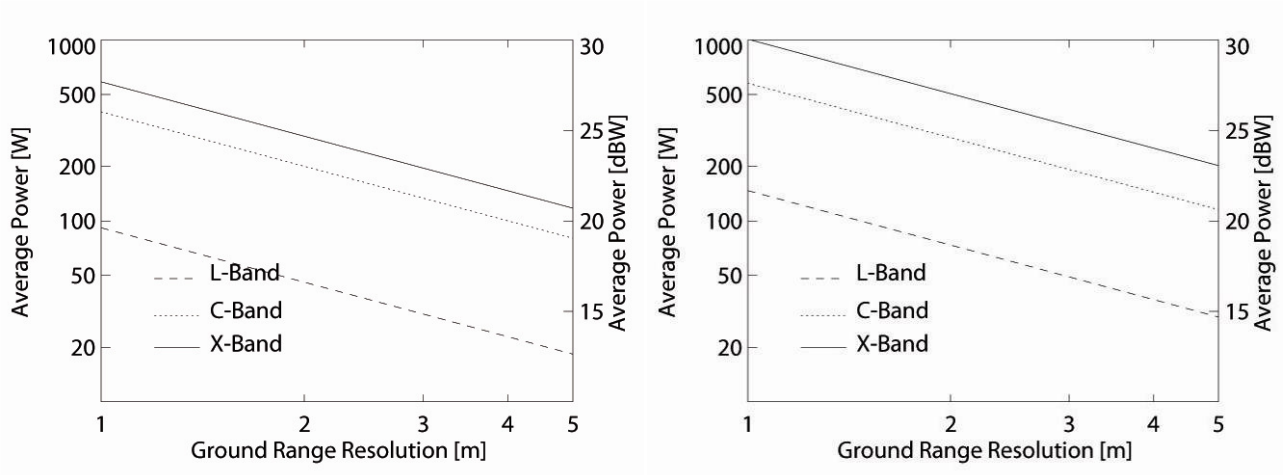

Fig. 5.6 L, C and X band Average Power vs. Range Resolution for 30 km (left) and 40 km (right) of swath

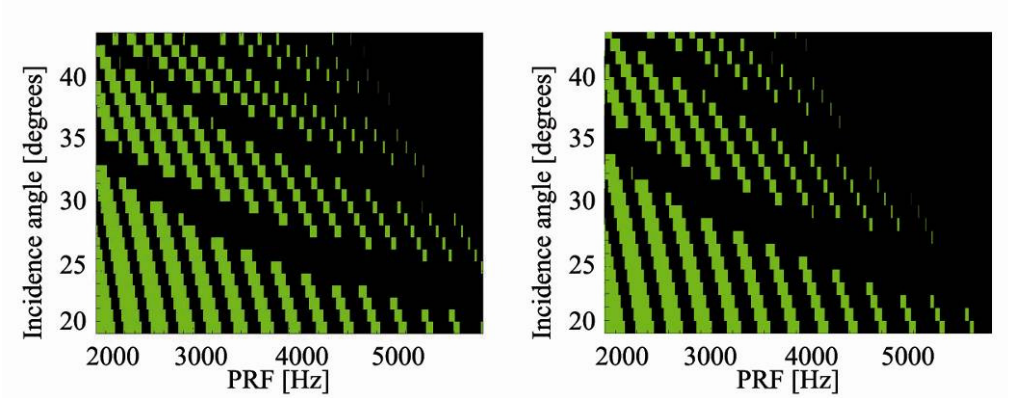

Fig. 5.7 Non interference PRF for 30 km (left) and 40 km (right) of swath

PRF values are illustrated in Fig. 5.7. With 40 km swath we only have a few PRF values higher than 5 KHz. This limitation becomes more significant as the incidence angle or the swath are increased.

In Fig. 5.8 compares the ASR for L, C, and X band for a range of swaths and a range of incidence angle. Notice that the darker and red zones (ASR near to -20dB, the limit specified) appear for high incidence angles. In L-Band we have needed to relax the requirements, increasing the antenna size in order to satisfy the ASR requirements. In spite of this, there are bad ASR values just up to 40 km swath.

In reference to power transmitted, lower frequency saves power if resolution is scaled with wavelength. Fig. 5.6 illustrates the relationship for both swaths.

Table 5.3 summarizes the result of the both SAR design and all the values that have been achieved.

As it is synthesized in Fig. 5.9 and Fig. 5.10**,** with these SAR configurations it is possible to develop a feasible sensor to respond to the necessity of the application described in chapter 5.1.

	L-Band	C-Band	X-Band	
f_0 [GHz]	1’3	5’3	9’65	
h [km]	511			
Incidence Angle [º]	[20, 45]			
Minimum Area [m^2]	[5’0-21’1]	[1’2-5’2]	[0’68-2’85]	
δx [m]	4	3		40 km swath
δRg [m]	3			
Antenna length [m]	8	6	6	
Antenna width [m]	3	1	0’56	
PRF [Hz]	[2098-4700]	[2643-5850]	[2666-5460]	
Average Power [W]	31	121	212	
δx [m]	3	2’5		30 km swath
δRg [m]	3			
Antenna length [m]	6	5	5	
Antenna width [m]	3’8	1’2	0’7	
PRF [Hz]	[2651-4655]	[3238-5793]	[3316-5752]	
Average Power [W]	34	121	196	

Table 5.3 Results for designed SAR configuration

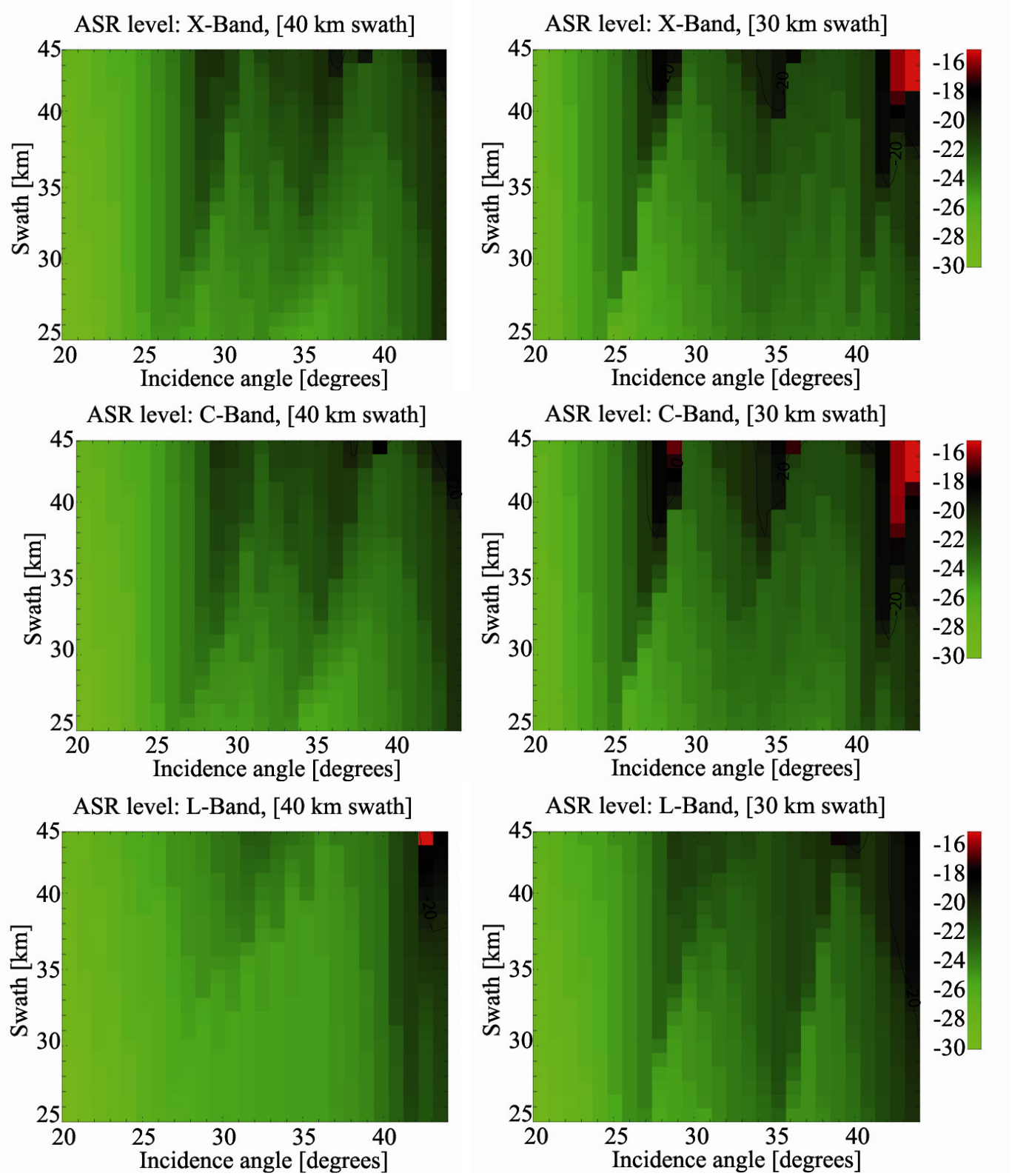

Fig. 5.8 Global ASR level for L, C and X band configurations and swaths from 45 to 25

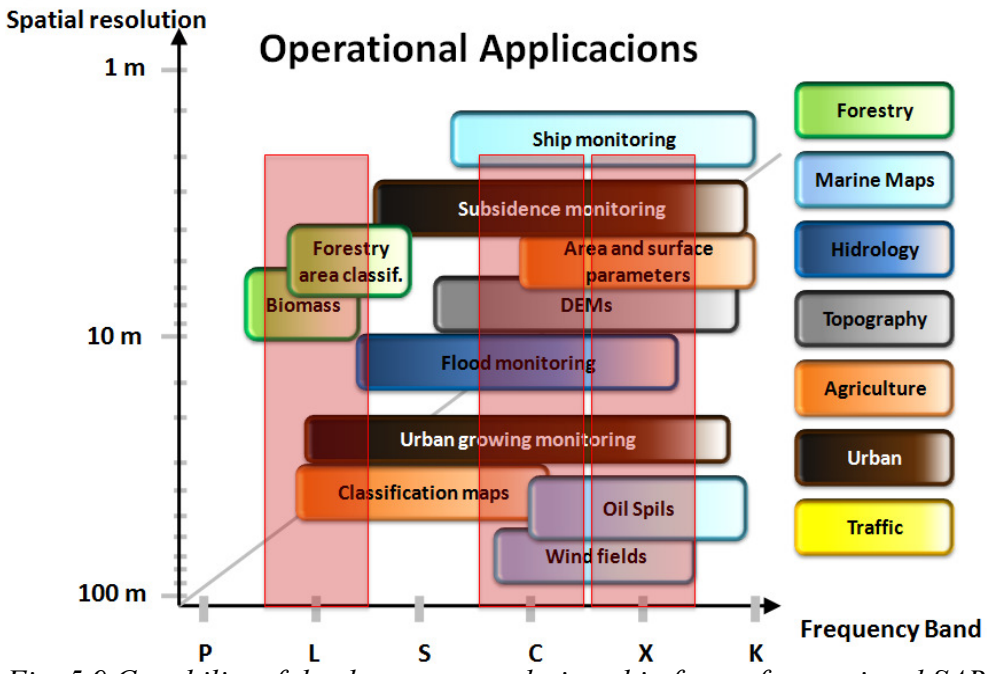

Fig. 5.9 Capability of the three sensors designed in front of operational SAR applications

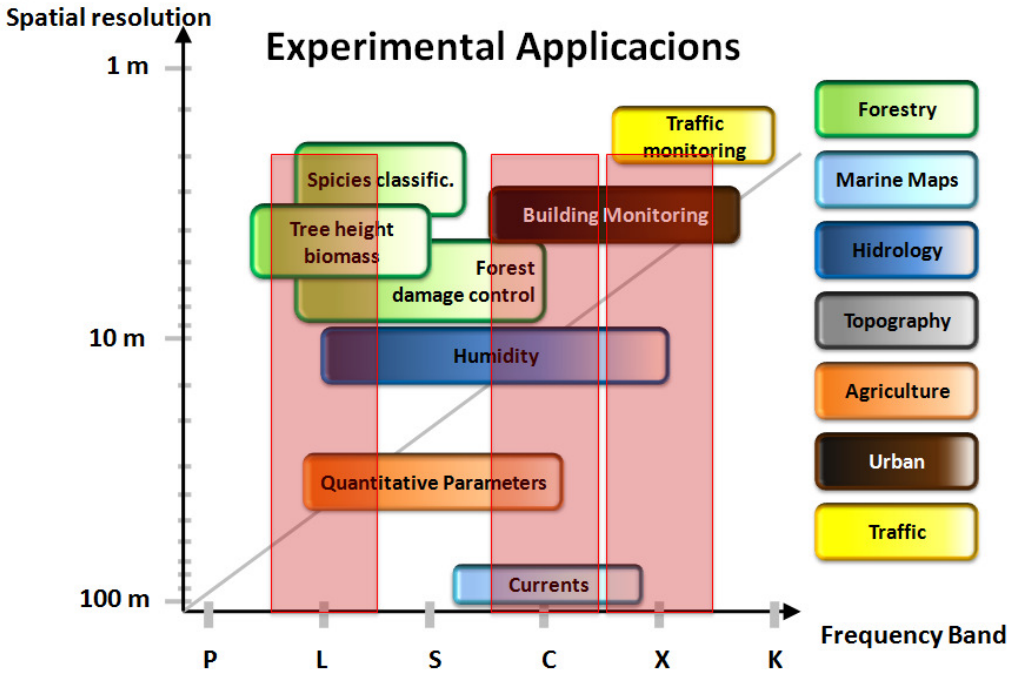

Fig. 5.10 Capability of the three sensors designed in front of experimental SAR applications

5.4 Data storage and down link.

A major constraint in the design of most current space-borne SAR systems is the available downlink data rate. For SAR systems, the swath width is either data rate limited or the system dynamic range has been degraded by reduced the number of bits per sample.

Considering the mission designed before the downlink capacity can be calculated with this

considerations:

- Quantization $N_b = \frac{SNR[dB] - 1.8}{6} = 5$ bits/sample
- Bandwidth $B_R = \frac{c}{2\delta R_g \sin\eta}$, incidence angle dependent
- PRF valid values (from 2666 to 5460) that optimize the .ASR.
- Swath width Sw = 40km
- Pulse time τ_p=30 μs

The required minimum slant range swath is approximately

$$\text{swath}_{\text{Slant}} \cong \text{swath} \cdot \sin(\eta) = 28Km$$

wich corresponds to a observation time of

$$\tau_w = 2\,\text{swath}_{\text{slant}}/c + \tau_p = 123\mu s$$

Assuming an oversampling factor g_{or} = 1.2, the sampling frequency is f_s = 84 Msamples/s. The number of samples per range line is therefore

$$N_r = f_s . \tau_w = 10{,}332 \text{ samples}$$

and the instantaneous data rate is

$$r_i = n_b . f_s = 420 \text{ Mbps}$$

Assuming the ADC output is buffered to achieve time expansion over the entire inter-pulse period, the average (sustained) real-time downlink data rate is

$$r_{DL} = \tau_w . r_i . PRF$$

and using the minimum and the maximum PRF values:

r_{DLmax}= 282,06Mbps
r_{DLmin}= 137,72 Mbps

Typically a downlink rate of these magnitudes cannot be achieved, since it would require a large downlink transmitter and antenna subsystem that cannot be accommodated within the platform resources, given the large mass and power requirements of the SAR. The alternative is to reduce the system performance by modifying either the system design or the data collection procedure. Among the available options are:

1- Increase the azimuth length (L_{az}) of the SAR antenna and reduce the PRF and/or the azimuth oversampling factor (g_{oa}) at the cost of increased mass and degraded azimuth resolution;

2- Reduce the system Bandwidth (B_R) and/or the range oversampling factor (g_{or}) at the cost of range resolution;

3- Reduce the Swath or change the imaging geometry to a steeper incidence angle (η) at the cost of ground coverage and increased geometric distorsion from foreshortening and layover effects

4- Reduce the quantization to fewer bits per sample (n_b) at the cost of increased distorsion noise and therefore a degraded impulse response function and radiometric calibration accuracy.

If an onboard processor were available to generate the image data in real time, the resolution degradation could be performed by multilook averaging, thus reducing the speckle noise in the process.

6 SUMMARY, CONCLUSIONS AND FUTURE LINES

6.1 Summary

The global context analyzed has showed us that nowadays, there is a trend toward designing satellite SAR missions more compact and in lower orbits. At this point, some questions appear in engineers minds: How small can we make a SAR system?

As the SAR system was designed to be boarded on a compact satellite, the antenna must be as small as possible. However, the price of reducing the antenna is:

- Reduced Swath (smaller images and revisit time increased)
- Reduced Ambiguity rejection
- More power required (without varying the altitude)

Because of this trade-off, the antenna size is not technological limited. However, a smaller antenna than the specified in Table 5.3 cannot be designed with the restrictions specified in Table 5.2.

Relaxing the ASR restriction and the swath width can help to design a smaller antenna but also can make the system data useless for most applications.

Bigger antennas are needed in lower frequency bands to satisfy the same restrictions. For this reason new missions planned are tending to board X-band systems.

For applications such as agricultural or forestry, L-band systems could be more appealing than C or X-band ones because of lower power is required. However, the penetration depth required for the application will determinate which should be the system frequency.

In terms of resolution, it seems that resolutions around a few meters are the maximum allowable for the system. For application with more precision like traffic monitoring, it could be necessary to reduce the satellite altitude in order to reduce power required and antenna size.

6.2 Conclusions

Compact platform are a good opportunity to design systems with good trade-offs between performance and costs than other big satellites missions.

According with the results of the designed SAR mission proposal, a SAR on a compact platform is feasible, with a certain degree. In order to establish a reference mission, a smaller satellite than TerraSAR-X could have problems to achieve the minimum

requirements for actual operational applications.

In the PCOT context, the design of a SAR system mission intended for cartography applications and much cheaper than TerraSAR-X mission it seems it would be not feasible with the current technology.

Analyzing the global context, Low Earth Orbit satellites are a global tool and it is useless to develop a SAR system only to use it in a concrete region. For this reason most of the missions are planned from partnerships in which research centers as the NASA (National Aeronautics and Space Administration) or the ESA (European Space Agency) are involved.

The solution to the PCOT SAR necessity could be other cheaper platforms as planes or zeppelins in order to design local missions.

6.3 Future lines

The study done could be extended by introducing new SAR concepts such as high resolution wide swath modes, new SAR antennas concepts working in other bands not mentioned, etc

In the mission design, satellite mass payload has not been determined and it could be interesting to study the antenna limit mass to establish its maximum weight.

Moreover, the satellite ground segment need to be designed: downlink antenna, control centre, mission control systems, planning and scheduling, simulator, payload data processing and archive.

The satellite altitude has been assumed from the recent missions so a extended study should include other types of compact missions such as unnamed and stratospheric platforms. They could be a good alternative to satellites for certain applications, or even a good complement.

Constellation missions are gaining special prominence in near future planned missions.

- Tandem-X (TerraSAR-X add-on for Digital Elevation Measurements) is a second, very similar spacecraft that will orbit in a close formation flight with TerraSAR-X, scheduled to be launched in 2009 [43].
- The Italian COSMO-SkyMed mission is a 4-spacecraft constellation, each equipped with X-band SAR. The first satellite was launched in June 2007, the second in December 2007, the third in October 2008 with the fourth satellite scheduled for launch in 2010.

A second version of the software could be programmed reducing some time process functions and introducing new features like orbit or downlink design

REFERENCES

[1] SEASAT Home Page http://southport.jpl.nasa.gov/scienceapps/seasat.html

[2] SIR-A Home Page http://southport.jpl.nasa.gov/scienceapps/sira.html

[3] SIR-B Home Page http://southport.jpl.nasa.gov/scienceapps/sirb.html

[4] Magellan Home Page http://www2.jpl.nasa.gov/magellan/fact.html

[5] European Space Agency Home Page http://earth.esa.int/ers/satconc/

[6] http://www.esa.int/esaEO/SEMGWH2VQUD_index_0_m.html

[7] http://envisat.esa.int/object/index.cfm?fobjectid=3760

[8] SIR-C Home Page http://southport.jpl.nasa.gov/sir-c/

[9] European Space Agency Home Page http://earth.esa.int/ers/

[10] Canadian Space Agency Home Page http://www.asc-csa.gc.ca/eng/satellites/radarsat1/default.asp

[11] Shuttle Radar Topography Mission Home Page http://www2.jpl.nasa.gov/srtm/

[12] Envisat Home Page http://envisat.esa.int/

[13] Japan Aerospace Exploration Agency Home Page http://www.jaxa.jp/projects/sat/alos/index_e.html

[14] Jörg Herrmann, Alejandra González Bottero, "TerraSAR-X Mission: The New Generation in High Resolution Satellites", Anais XIII Simpósio Brasileiro de Sensoriamento Remoto, Florianópolis, Brasil, 21-26 abril 2007, INPE, Pages: 7063-7070.

[15] Rolf Werninghaus, Wolfgang Balzer, Stefan Buckreuss, Josef Mittermayer, Peter Mühlbauer , "TerraSAR-X Mission", http://www.dlr.de/tsx/documentation/EUSAR-TX-Mission.pdf

[16] Radarsat Home Page http://www.radarsat2.info/

[17] OHB-System AG, Universitätsallee 27–29, The SAR-LUPE Programm-An Industrial View -Security and Defence Aspects of Space:The Challenges for EUAthens, Greece, May 8-9, 2003, http://ec.europa.eu/comm/space/doc_pdf/merkle.pdf

[18] OHB-System AG, Universitätsallee 27–29, "SAR-Lupe, The innovative program for satellite-based radar reconnaissance" http://www.ohb-system.de/pdf/sar-lupe-broschure.pdf

[19] SAR-Lupe Constellation
http://directory.eoportal.org/pres_SARLupeConstellation.html

[20] JianBing 5 (YaoGan WeiXing 1/3) Synthetic Aperture Radar Satellite
http://www.sinodefence.com/strategic/spacecraft/jianbing5.asp

[21] Tuyuan Technologies "Surveyor" Satellite Constellation
http://www.spaceref.com/news/viewpr.html?pid=14919

[22] China Plans Commercial SAR EO Constellation"
http://news.eoportal.org/eomissions/040907_surveyo.html

[23] Alcatel Alenia Space Radar System For The Korean EO Sat Kompsat-5, http://www.spacemart.com/reports/Alcatel_Alenia_Space_Radar_System_For_The_Korean_EO_Sat_Kompsat_5.html

[24] Ian Hønstvet , Ian Encke , David Hall , Yvonne Munro "ASTROSAR-LITE – A RADAR SYSTEM FOR THE TROPICS" Anais XIII Simpósio Brasileiro de Sensoriamento Remoto, Florianópolis, Brasil, 21-26 abril 2007, INPE, p. 4907-4913.

[25] Attema, E., 2005. Mission Requirements ,Document for the European Radar Observatory Sentinel-1, ESA, ES-RS-ESA-SY-0007, Noordwijk, The Netherlands, http://esamultimedia.esa.int/docs/GMES/GMES_SENT1_MRD_1-4_approved_version.pdf

[26] Reinhard Schröder, Jürgen Puls, Irena Hajnsek, Fritz Jochim, Thomas Neff, Janio Kono,Waldir Renato Paradella, Mario Marcos Quintino da Silva, Dalton de Morisson Valeriano, Maycira Pereira Farias Costa, "MAPSAR: a small L-band SAR mission for land observation", Acta Astronáutica 56 (2005), Pages: 35 – 43

[27] Vincent, N.; Gaillard, D.; Banos, T.; "Small satellite system for civilian radar imagery application", Geoscience and Remote Sensing Symposium Proceedings, 1998. IGARSS '98. 1998 IEEE International, Volume 1, 6-10 July 1998 Pages: 274 - 276 vol.1

[28] Aguttes, J.P., "High resolution (metric) SAR microsatellite, based on the CNES MYRIADE bus", Geoscience and Remote Sensing Symposium, 2001. IGARSS '01. IEEE 2001 International, Volume 1, 9-13 July 2001 Pages:224 - 226 vol.1

[29] Albert Aguasca Solé, Antoni Broquetas Ibars, Adriano Camps Carmona, Xavier Fàbregas Cànovas, Albert García Mondéjar, Paco López Dekker, Carlos López Martínez, Jordi Mallorquí Franquet, SARMISP: " SAR Mission on Small Platforms" December 2008

[30] Ulaby, F.T., R.K. Moore and A.K. Fung (1982). Microwave Remote Sensing, Vol.

2, Addison-Wesley, Reading, MA.

[31] Cutrona , L.J. (1970) "Synthetic Aperture Radar", Chapter 23 in Radar Handbook (Skolnik, M.I.,ed.) McGraw-Hill, New York

[32] John C. Curlander and Robert N. McDonough (1991)"Synthetic Aperture Radar – systems and Signal Processing" Wiley series in remote sensing.

[33] http://www.mityc.es/Telecomunicaciones/Secciones/Espectro/cnaf/

[34] Boerner W.-M., Mott H., Lunenburg E., Livingstone C., Brisco B., Brown R. J., Patterson J. S. Polarimetry in Remote Sensing: Basic and Applied Concepts, chapter 5: in Manual of Remote Sensing, Volume 2: Principles and Applications of Imaging Radar. Wiley, 3rd edition, 1998.

[35] Sauer, S.; Ferro-Famil, L.; Reigber, A.; Pottier, E., "Multibaseline POL-InSAR analysis of urban scenes for 3D modeling and physical feature retrieval at L-band," Geoscience and Remote Sensing Symposium, 2007. IGARSS 2007. IEEE International , vol., no., pp.1098-1101, 23-28 July 2007

[36] Bayman, R.W. and P.A. McInnes (1975). "Aperture Size and Ambiguity Constraints for Synthetic Aperture Radar," IEEE 1975 Inter. Radar Conf., pp.49-504

[37] Kühbauch, W.; Hawlitschka, S., "Remote Sensing - A Future Technology in Precision Farming," Pol-InSAR 2003, Frascati, Italy, January 2003

[38] C. Lin and R. Päivinen, "Forestry user requirement assessment – the SAR for Agriculture and Forestry in Europe (SAFE) project experiences and results," Retrieval of Bio- and Geo-Physical Parameters from SAR Data for Land Applications Workshop ESTEC, 21-23 October 1998

[39] Vincent Kerboal, Fabrice Collard "SAR-Derived Coastal and Marine Applications: From Research to Operational Products", IEEE Journal of Oceananic Engineering, Vol. 30, Nº 3, July 2005

[40] Lee, J., Schuler, T., Krogager, E. & Kasilingam, W. "On the estimation of radar polarization orientation shifts induced by terrain slopes", Geoscience and Remote Sensing, IEEE Transactions on, vol. 40, pp 30-41 , 2002.

[41] L. Tsang, J.A. Kong and R.T. Shin. "Theory of Microwave Remote Sensing", Wiley Interscience Publication, New York, 1985.

[42] Zebker H A and Goldstein R M 1986 Topographic mapping from interferometric synthetic aperture radar observations J. Geophys. Res. 91 4993–9

[43] Tandem-X http://www.infoterra.de/terrasar-x/tandem-x-mission.html

[44] COSMO-Skymed http://www.deagel.com/C3ISTAR-Satellites/COSMO-SkyMed_a000256001.aspx

APPENDIX A. IDL ROUTINES

1. mysar & sarstruct

```
function mysar,h_sar=h_sar,f0=f0,gamma=gamma, tau_p=tau_p, az_res=az_res,
grg_res=grg_res,L_az=L_az,L_el=L_el,$
      swath=swath,PRF=PRF, sigma_noise=sigma_noise,ASR=ASR, P_avg=P_avg

  mysar=sarstruct()

  mysar.h_sar=h_sar
  mysar.f0=f0
  mysar.gamma=gamma

  if keyword_Set(tau_p) then mysar.tau_p=tau_p
  if keyword_Set(az_res) then mysar.az_res=az_res
  if keyword_Set(grg_res) then mysar.grg_res=grg_res
  if keyword_Set(L_az) then mysar.L_az=L_az
  if keyword_Set(L_el) then mysar.L_el=L_el
  if keyword_Set(swath) then mysar.swath=swath
  if keyword_Set(sigma_noise) then mysar.sigma_noise=sigma_noise
  if keyword_Set(ASR) then mysar.ASR=ASR
  if keyword_Set(PRF) then mysar.PRF=PRF
  if keyword_Set(P_avg) then mysar.P_avg=P_avg

  return,mysar

end



function sarstruct

 dh = { SAR_PARS,                          $ ; structure tag
         h_sar  : 0.0,                     $ ; fly height
         grg_res  : 0.0,                   $ ; Ground range resoluton
         az_res : 0.0,                     $
         swath : 0.0,                      $
         sigma_noise : 0.0 ,               $
         ASR: 0.0,                         $ ;Ambiguity signal ratio
         gamma : fltarr(2),                $
         L_az : 0.0,                       $ ;Antenna length (azimuth)
         L_el : 0.0,                       $ ;Antenna width (alevation)
         eta_ant : 0.0,                    $ ;Radiation efficiency
         ap_eff : 0.0,                     $
         P_av : 0.0,                       $ ; Average transmmitted power
         PRF : fltarr(2),                  $
         tau_p :0.0,                       $
         f0 : 0.0 }                        $; wavelength
  return, dh

end
```

2. orbit_vel & areamin

```
function orbit_vel,h
  ;; Calculate orbital velicity assuming circular orbit
  Me = 5.9742e24
  Re = 6.378e6
  G= 6.67300e-11
  vel= sqrt(G*Me/(Re+h))
  return, vel
end

function areamin, sar, GAMMA=GAMMA,h=h, f0=f0, plot=plot

      if not keyword_Set(GAMMA) then gamma=sar.gamma;look angle
      if not keyword_Set(f0) then f0=sar.f0
      if not keyword_Set(h) then h=sar.h_sar


      c=3e8
      R_earth=6371e3
      R_s=6371e3 + sar.h_sar  ;From earth-center to sensor
      R_t=6371e3              ;From earth-center to target

      area=fltarr(max(gamma))
      R_c=fltarr(max(gamma))

      for i=min(gamma),(max(gamma)-1) do begin


            i_gamma=i
            i_gamma_rad=i_gamma*!PI/180

            eta_c=asin(R_s/R_t*sin(i_gamma_rad)) ;boresight incidence
            angle
            R_c[i]=R_s*cos(eta_c)-sqrt(R_t^2-R_s^2+R_s^2*cos(eta_c)^2)
            ;From sensor to target

            v=orbit_vel(h)

            area[i]=4/f0*R_c[i]*v*tan(eta_c)
      endfor

      ;print,"R=", R_c
      plot,area, xrange=[min(gamma),max(gamma)], xstyle=1,xtitle=
      'Incidence angle / deg', ytitle= 'area [mxm]'
      if keyword_Set(plot) then begin
            SET_PLOT, 'PS'
            ; Set the filename:
            DEVICE, FILENAME='area.ps'

            plot,area, xrange=[min(gamma),max(gamma)], xstyle=1,xtitle=
            'Incidence angle / deg', ytitle= 'area [mxm]'
            DEVICE, /CLOSE
            ; Return plotting to Windows:
            SET_PLOT, 'win'

      endif
return, area

end
```

3. PRFbad

```
function prfbad, sar, PRF=PRF,GAMMA=GAMMA,swath=swath, tau_p=tau_p,
            tau_rp=tau_rp, xres=xres, yres=yres, plot=plot, $
            epsfile=epsfile, paperstyle=paperstyle

;; this function prints a "map" whith the non-interference PRFs

      if not keyword_Set(PRF) then prf=sar.prf
      if not keyword_Set(GAMMA) then gamma=sar.gamma;look angle
      if not keyword_Set(swath) then swath=sar.swath
      if not keyword_Set(tau_p) then tau_p=sar.tau_p
      if not keyword_Set(tau_rp) then tau_rp=tau_p
      if not keyword_Set(xres) then xres=1
      if not keyword_Set(yres) then yres=1


      c=3e8
      R_earth=6371e3
      R_s=6371e3 + sar.h_sar  ;From earth-center to sensor
      R_t=6371e3              ;From earth-center to target
      h=sar.h_sar
      n_pts=1000
      nh=1000


      xdim=xres*double(max(prf)-min(prf));+1
      ydim=yres*(max(gamma)-min(gamma));+1
      status=fltarr(xdim,ydim); PRF error value
      status2=fltarr(xdim,ydim) ; interference PRFs
      status3=fltarr(xdim,ydim) ; non interference PRFs


      for i=0,yres*(max(gamma)-min(gamma)-1) do begin

            i_gamma=min(gamma)+i/yres
            i_gamma_rad=i_gamma*!PI/180

            eta_c1=asin(R_s/R_t*sin(i_gamma_rad)) ;boresight incidence
            angle
            slswath=sin(eta_c1)*swath ;slant range swath
            R_c1=R_s*cos(eta_c1)-sqrt(R_t^2-R_s^2+R_s^2*cos(eta_c1)^2)
            ;From sensor to target
            R_c=R_c1+findgen(n_pts)/n_pts*slswath-slswath/2 ; Slant Range
            R_1= min(R_c)
            R_N= max(R_c)

            for j=0,xres*(max(PRF)-min(PRF)-1) do begin

                  ;;;;;;;;;;;;;;;;;;;;;;
                  ;TRANSMIT INTERFERENCE;
                  ;;;;;;;;;;;;;;;;;;;;;;


                  i_prf=min(prf)+j/xres

                  if ((((2*R_1*i_prf/c - floor(2*R_1*i_prf/c))/i_prf gt
                  (tau_p+tau_rp)) $
                   or ((2*R_N*i_prf/c - floor(2*R_N*i_prf/c))/i_prf lt
                  (1/i_prf-tau_rp))) $
```

```
                and (floor(2*R_N*i_prf/c) eq floor(2*R_1*i_prf/c)))
                then begin ;non interference PRFs

                      status[(i_prf-min(prf))*xres,(i_gamma-
                      min(gamma))*yres]=0
                      status2[(i_prf-min(prf))*xres,(i_gamma-
                      min(gamma))*yres]=0
                      status3[(i_prf-min(prf))*xres,(i_gamma-
                      min(gamma))*yres]=i_prf


                endif else begin ;PRF transmit interference
                      status[(i_prf-min(prf))*xres,(i_gamma-
                      min(gamma))*yres]=1
                      status2[(i_prf-min(prf))*xres,(i_gamma-
                      min(gamma))*yres]=0.5
                      status3[(i_prf-min(prf))*xres,(i_gamma-
                      min(gamma))*yres]=0


                endelse

                ;;;;;;;;;;;;;;;;;;;
                 ;NADIR INTERFERENCE;
                ;;;;;;;;;;;;;;;;;;;

                kk=2*(dindgen(nh))-nh

                nadir1=2*h/c+kk/i_prf
                nadir2=2*h/c+2*tau_p+kk/i_prf

                if(total((nadir1 lt (2*R_N/c))*(nadir2 gt (2*R_1/c)))
                eq 1) then begin
                      status[(i_prf-min(prf))*xres,(i_gamma-
                      min(gamma))*yres]+=2
                      status2[(i_prf-min(prf))*xres,(i_gamma-
                      min(gamma))*yres]=0.5
                      status3[(i_prf-min(prf))*xres,(i_gamma-
                      min(gamma))*yres]=0

                endif

          endfor


    endfor


    status2[(i_prf-min(prf))*xres,(i_gamma-min(gamma))*yres]=1; mark
    the maximum level at 1 (red) to paint the interference PRF black
    (0.5)
    if keyword_set(plot) then begin
          !P.BACKGROUND=0
          !P.COLOR=255
          if keyword_set(epsfile) then begin
                SET_PLOT, 'PS'
                DEVICE, FILENAME='minASR.ps'
          endif
          if keyword_set(paperstyle) then begin
                !P.BACKGROUND=255
                !P.COLOR=0
```

```
            endif
            !P.MULTI = 0
      image,status2,xmin=min(PRF),xmax=max(PRF),ymin=min(GAMMA),ymax=max(
      GAMMA),NOCOLORBAR=1,XTITOL='PRF [Hz]',YTITOL='Incidence angle
      [degrees]',PAPERSTYLE=1, charsize=1.5 ;, pngfile='prfbad2.png'
      if keyword_set(epsfile) then begin
            DEVICE, /CLOSE
            SET_PLOT, 'win'
      endif
      endif

      return, status3

end
```

4. sarsens

```
function sarsens, grg_res=grg_res, az_res=az_res, NF=NF, Tant=Tant,
            h_sar=h_sar, Gamp=Gamp, ADCrange=ADCrange, ADCnbits=ADCnbits,
            sigma_noise=sigma_noise, gamma=gamma, f0=f0, swath=swath,
            eta_ant=eta_ant, P_avg=P_avg, silent=silent, L_el=L_el,
            ap_eff=ap_eff, pulse_diversity=pulse_diversity

;;KEYWORDS
;;grg_res: ground range resolution (10)
;;az_res: aziuth resolution (10)
;;NF: receiver Noise Figure (7 dB)
;;f0: carrier frequency (5.3e9)
;;h_sar: platform altitude in m (780e3)
;;gamma: incidence angle, in degree (23)
;;eta_ant: radiation efficiency (0.5)
;;P_av: Average power. If not set it is calculated to achieve a given
sensitivity
;;L_el: if not set this returns the calculated dimension of the
;;antenna in elevation, otherwise forces it
;;swath: if not set it is calculated as the maximum non ambiguous.
;;       If it is passed and it is too large, it is modified.
;;ap_ef: aperture efficiency, set to 0.5 for ERS/ENVISAT
;;pulse_diversity: this option allows alternating waveforms to
;;resolve range ambiguities and introducing autoclutter

;if not keyword_set(grg_res) then grg_res=3.
      if not keyword_set(az_res) then az_res=3.
      if n_elements(NF) eq 0 then NF=7.
      if not keyword_Set(f0) then f0=9.65e9
      if not keyword_set(h_sar) then h_sar=500e3
      if not keyword_set(Tant) then Tant=300
      if not keyword_set(sigma_noise) then sigma_noise=-22
      if not keyword_set(gamma) then gamma=20
      if not keyword_Set(eta_ant) then eta_ant=0.5
      if not keyword_Set(ap_eff) then ap_eff=0.5
      ;;constants
      c=3e8                          ;Speed of light
      j=complex(0,1)
      kb=1.38e-23     ;Boltzman constant

      R_earth=6371e3
      R_s=6371e3 + h_sar          ;From earth-center to sensor
      R_t=6371e3                    ;From earth-center to targe


      ;;derived constants
      lambda_0=c/f0                  ;Carrier wavelength
      k_0=2*!pi/lambda_0
      ;; Look angle
      gamma_1=!dtor*min(gamma)
      eta_c1=asin(R_s/R_t*sin(gamma_1)) ;Boresight incidence angle

      ;;Lets calculate the necessary bandwidth
      srg_res=grg_res*sin(eta_c1)  ;Slant-range resolution

      ;;Therefore the chirp bandwidth is
      ;; srg_res=c/(2*NBW)
      NBW=c/2/srg_res
      R_1=h_sar/cos(gamma_1)
```

```
;;From the azimuth resolution we can derive the antenna length in
;;stripmap mode
L_az=2*az_res
;;we can correct it by a spotlight factor...


;;TODO!!!!!!!

;;azimuth beamwidth
gamma_az=lambda_0/L_az

;;Doppler bandwidth
v_orb=orbit_vel(h_sar)
B_dop=v_orb*gamma_az*2/lambda_0
PRFmin=B_dop
PRTmax=1./PRFmin
Ramb=c/2*PRTmax

;;Non ambiguous swath:
swath_amb=(Ramb)/sin(eta_c1)
if not keyword_set(silent) then print,'max unambiguous  swath
width',swath_amb
if not keyword_Set(swath) then begin
      ;;If swath is not specified then set to max unambigous
      swath=swath_amb
endif else begin
      if (swath gt (Ramb)/sin(eta_c1)) and (not
      keyword_Set(pulse_diversity))  then begin
            ;;If swath is set but too large then it is adjusted
            swath=swath_amb
            if not keyword_set(silent) then print, "Adjusting swath
            to maximum allowable"
      endif
endelse

;;Elevation beamwidth adjusted to swath to get antenna width
gamma_el=2*asin(cos(eta_c1)*swath/2/R_1)
L_el_swath=lambda_0/gamma_el/ap_eff

;;Same adjusted to ambiguous swath
gamma_el_amb=2*asin(cos(eta_c1)*swath_amb/2/R_1)
L_el_amb=lambda_0/gamma_el_amb/ap_eff

if not keyword_set(L_el) then begin
      L_el=L_el_amb
endif else begin
      if (L_el_amb gt L_el) and not keyword_set(silent) then begin
            print, 'Antenna width is too small!'
      endif
endelse
if not keyword_set(silent) then print, "L_el=",L_el

G_t=ap_eff*4*!pi*(L_el/lambda_0)*(L_az/lambda_0)

if not keyword_set(silent) then print,"Antenna gain", db(G_t)

Tsys=Tant+(db2lin(1.0*NF)-1)*290
N=kb*NBW*Tsys
;;         eta_ant P_av Gt^2 lambda_0^3 dRg sigma_0
;; SNR = ----------------------------------------
;;          2 (4*!pi)^3 R^3 k Tsys v_sar
```

```
      if keyword_set(P_avg) then begin
            if not keyword_set(silent) then print,"Calculating sigma_ne"
            sigma_noise=2*(4*!pi*R_1)^3*kb*Tsys*v_orb/
            (P_avg*G_t^2*lambda_0^3*g           rg_res)
            return, db(sigma_noise)
      endif else begin
            if not keyword_set(silent) then print,"Calculating
            P_avg"
            P_avg=2*(4*!pi*R_1)^3*kb*Tsys*v_orb/
            (G_t^2*lambda_0^3*grg_res*db2lin(sigma_noise))
            return, P_avg
      endelse
      return,db(1)
end
```

5. saramb

```
function saramb, sar, elbeam=elbeam, azbeam=azbeam, swath=swath, PRF=PRF,
                 L_el=L_el, L_az=L_az,AASR=AASR,gamma=gamma,
                 az_reso=az_reso

      ;; Options
      if not keyword_set(elbeam) then elbeam='uniform'
      if not keyword_set(azbeam) then azbeam='uniform'
      if not keyword_set(swath) then swath=sar.swath
      if not keyword_set(PRF) then PRF=sar.prf
      if not keyword_set(L_el) then L_el=sar.L_el
      if not keyword_set(L_az) then L_az=sar.L_az
      if not keyword_Set(gamma) then gamma=min(sar.gamma)
      if swath eq 0 then swath=30e3
      if not keyword_set(az_reso) then az_reso=L_az/2 ;"az_reso" is the
      azimuth resolution considered in the procwindow.
      ;If not considered put the nominal Laz/2
      ;;Constants
      c=3e8
      j=complex(0,1)
      n_amb=16
      n_pts=1000
      ;geometry
      R_earth=6371e3
      R_s=6371e3 + sar.h_sar        ;From earth-center to sensor
      R_t=6371e3                    ;From earth-center to targe

      gamma=gamma*!PI/180

      eta_c1=asin(R_s/R_t*sin(gamma)) ;Boresight incidence angle
      ;swath in slant range
      slswath=swath*sin(eta_c1)
      lambda0=c/sar.f0

      ;;;;;;;;;;;;;;;;;;;;;;;;;;;;;;;;;;;;;;;;;;;;;;;;;;;;;;;;;;;;;;;;;;;;
      ;;RANGE AMBIGUITIES;;;;;;;;;;;;;;;;;;;;;;;;;;;;;;;;;;;;;;;;;;;;;;;;;
      ;;;;;;;;;;;;;;;;;;;;;;;;;;;;;;;;;;;;;;;;;;;;;;;;;;;;;;;;;;;;;;;;;;;;

      ;;find range to reference target at center of beam

      R_c1=R_s*cos(gamma)-sqrt(R_t^2-R_s^2+R_s^2*cos(gamma)^2) ;From
      sensor to target

      ;print, "R_c",R_c1
      R_c=R_c1+findgen(n_pts)/n_pts*slswath-slswath/2
      R_amb=(1+fltarr(1,n_amb))##R_c+(transpose([-
      reverse(1+indgen(n_amb/2)),1+indgen(n_amb/2)]))##(fltarr(n_pts)+1)*
      c/2./PRF
      gamma_amb=acos((R_amb^2+R_s^2-R_t^2)/(2*R_amb*R_s))

      gamma_c=acos((R_c^2+R_s^2-R_t^2)/(2*R_c*R_s))
      ;print,"gamma_amb =", gamma_amb/!dtor
      eta_amb=asin(R_s*sin(gamma_amb)/R_t)
      eta_c=asin(R_s*sin(gamma_c)/R_t)
      ;print, "eta=", eta_amb/!dtor

      case elbeam of
            'uniform': begin
                  bp2_amb=(sincbp(gamma_amb-gamma,L_el,sar.f0))^2
```

```
            bp2_target=(sincbp((1+fltarr(1,n_amb))##gamma_c-
            gamma,L_el,sar.f0))^2
      end
      'circ_uniform': begin
            bp2_amb=(circbp(gamma_amb-gamma,L_el,sar.f0))^2
            bp2_target=(circbp((1+fltarr(1,n_amb))##gamma_c-
            gamma,L_el,sar.f0))^2
      end
      'hanning': begin
            bp2_amb=(hanningbp(gamma_amb-gamma,L_el,sar.f0))^2
            bp2_target=(hanningbp((1+fltarr(1,n_amb))##gamma_c-
            gamma,L_el,sar.f0))^2
      end
      else : begin
            bp2_amb=(sincbp(gamma_amb-gamma,L_el,sar.f0))^2
            bp2_target=(sincbp((1+fltarr(1,n_amb))##gamma_c-
                  gamma,L_el,sar.f0))^2
      end
endcase

badpoints=where(~finite(bp2_amb),n_bad)
badpoints=where(~finite(gamma_amb),n_bad)
if n_bad gt 0 then bp2_amb[badpoints]=0

rangeamb=(bp2_amb/bp2_target)*
(((1+fltarr(1,n_amb))##R_c)/(R_amb))^3
;;Return swath positions, integrated RASR and max RASR

res=[[R_c],[total(rangeamb,2)],[max(rangeamb,dimension=2)]]
;window,xsize=800,ysize=600,TITLE='RASR', /FREE
;iplot,(res[*,0])/1000,db(res[*,1]), xtitle='Rc[Km]', ytitle='RASR
[dB]'

;;;;;;;;;;;;;;;;;;;;;;;;;;;;;;;;;;;;;;;;;;;;;;;;;;;;;;;;;;;;;;;;;;;
;;AZIMUTH AMBIGUITIES;;;;;;;;;;;;;;;;;;;;;;;;;;;;;;;;;;;;;;;;;;;;;;
;;;;;;;;;;;;;;;;;;;;;;;;;;;;;;;;;;;;;;;;;;;;;;;;;;;;;;;;;;;;;;;;;;;

;; Satellite velocity (approx)
v_sar_approx=orbit_vel(sar.h_sar)
;;Lets take 20 seconds
t_span=30.*5.3e9/sar.f0
nazpts=20000
t=(findgen(nazpts)/nazpts-0.5)*t_span
theta_az=(t*v_sar_approx*R_earth/R_s)/mean(R_c)
dop=theta_az*2*v_sar_approx/lambda0
case azbeam of
      'uniform': begin
            azbp2=sincbp(theta_az,L_az,sar.f0)^2
      end
      'circ_uniform': begin
            azbp2=circbp(theta_az,L_az,sar.f0)^2
      end
      'hanning': begin
            azbp2=hanningbp(theta_az,L_az,sar.f0)^2
      end
      else : begin
            azbp2=sincbp(theta_az,L_az,sar.f0)^2
      end
endcase
;plot,dop,(azbp2)
inwindow=where(abs(dop) le V_sar_approx/az_reso/2,howmany)
```

```
        outwindow=where(abs(dop) le PRF/2,howmany2)
        kk=max(azbp2,whmax)
        procwin=hanning(howmany,alpha=0.54)
        if howmany gt 0 then Pmain=total(procwin*azbp2[inwindow]) else
        Pmain=0
        nwin=floor(nazpts/howmany2-1)/2
        Ptot=0
        for i_win=-nwin,nwin do
        Ptot=Ptot+total(procwin*azbp2[inwindow+i_win*howmany2])
        Pamb=Ptot-Pmain
        AASR=Pamb/Pmain

        ;;print,"AASR=",db(AASR)

        return, res
end
```

6. bestPRF

```
function bestPRF, sar, GAMMA=GAMMA, SWATH_MAX=SWATH_MAX, PRF=PRF,
            asr_thres=asr_thres, elbeam=elbeam, azbeam=azbeam,
            nprfpts=nprfpts, plot=plot, epsfile=epsfile,
            swathres=swathres, swath_min=swath_min,
            paperstyle=paperstyle, L_el=L_el, L_az=L_az, az_reso=az_reso

      ;function to find the valid PRF values that minimize PRF
      ambiguities
      ;PRF: range of possible PRFs
      ;GAMMA: range of possible look angle values.
      ;SWATH: maximum swath wanted

      if not keyword_Set(GAMMA) then gamma=sar.gamma ;look angle
      if not keyword_Set(swath_max) then swath_max=sar.swath
      if not keyword_Set(asr_thres) then asr_thres=-20
      if not keyword_Set(nprfpts) then nprfpts=100
      if not keyword_Set(swathres) then swathres=10000
      if not keyword_Set(swath_min) then swath_min=20e3
      ;if not keyword_set(elbeam) then elbeam='uniform'
      if not keyword_set(azbeam) then azbeam='uniform'
      if not keyword_Set(L_el) then L_el=sar.L_el
      if not keyword_Set(L_az) then L_az=sar.L_az
      if not keyword_set(az_reso) then az_reso=L_az/2


      nswaths=round((swath_max-swath_min)/swathres+1)

      nprfs=max(prf)-min(prf)
      prfs=round(min(prf)+(max(prf)-min(prf))*findgen(nprfpts)/(nprfpts))

      ngamma=max(gamma)-min(gamma)+1
      gammas=findgen(ngamma+1)+min(gamma)

      PRFvalid=fltarr(nprfs,ngamma)
      BestPRFs=fltarr(nswaths,ngamma)
      BestGAMMAs=fltarr(nprfs)
      RASR=fltarr(nswaths, nprfs,ngamma)
      RASR1=fltarr(nswaths, nprfs,ngamma)
      RASR2=fltarr(nswaths, nprfs,ngamma)
      hanning_mask=fltarr(nswaths, nprfs,ngamma)
      AASR=fltarr(nswaths,nprfs,ngamma)
      AASR_mask=fltarr(nswaths,nprfs,ngamma)
      AMB_level=fltarr(nswaths,nprfs,ngamma)
      ilevel=fltarr(nswaths,ngamma)
      RASRbest=fltarr(nswaths,ngamma)
      RASRbest1=fltarr(nswaths,ngamma)
      RASRbest2=fltarr(nswaths,ngamma)
      AASRbest=fltarr(nswaths,ngamma)

      for iswath=swath_max, swath_min, -swathres do begin
            i_swath=(iswath-swath_min)/swathres
            print, 'Definint PRF valides pel swath de', iswath/1000, 'km'
            PRFvalid=prfbad(sar, PRF=prf, GAMMA=GAMMAs, SWATH=iSWATH) ;
            Non interference PRFs

            for i_gamma=0, ngamma-1 do begin
                  print, 'ASRs for look angle of ', i_gamma+min(gamma),
                  '° & swath of',iswath/1000, 'km'
                  for i_prf=0,nprfpts-1 do begin
```

```
                iprf=(prfs[i_prf]-min(prf))

                if PRFvalid[iprf,i_gamma] ne 0 then begin ; valid PRF
                      AMB=saramb(sar, L_az=L_az, L_el=L_el,
                      PRF=PRFvalid[iprf,i_gamma], GAMMA=
                      gammas[i_gamma], SWATH=iswath, AASR=thisaasr,
                      az_reso=az_reso, elbeam='uniform', azbeam=azbeam)
                      AMB2=saramb(sar, L_az=L_az,L_el=L_el,
                      PRF=PRFvalid[iprf,i_gamma], GAMMA=
                      gammas[i_gamma], SWATH=iswath, AASR=thisaasr,
                      az_reso=az_reso, elbeam='hanning', azbeam=azbeam)

                      AASR[i_swath,iprf,i_gamma]=db(thisaasr)

                      RASR1[i_swath,iprf,i_gamma]=db(max(AMB[*,1]));
                      amb finestra uniforme
                      RASR2[i_swath,iprf,i_gamma]=db(max(AMB2[*,1]));
                      amb finestra hamming

                      ;em quedo amb el RASR que dona millor resultat de
                      les dues finestres
                      if RASR1[i_swath,iprf,i_gamma] gt
                      RASR2[i_swath,iprf,i_gamma] then begin

                            RASR[i_swath,iprf,i_gamma]=
                            RASR2[i_swath,iprf,i_gamma]
                            hanning_mask[i_swath,iprf,i_gamma]=1
                      endif else begin

                            RASR[i_swath,iprf,i_gamma]=
                            RASR1[i_swath,iprf,i_gamma]
                      endelse
                      ;em quedo amb el pitjor rebuig com a pitjor cas.
                      if AASR[i_swath,iprf,i_gamma] gt
                      RASR[i_swath,iprf,i_gamma] then begin
                            AMB_level[i_swath,iprf,i_gamma]=
                            AASR[i_swath,iprf,i_gamma]
                            AASR_mask[i_swath,iprf,i_gamma]=1
                      endif else begin
                            AMB_level[i_swath,iprf,i_gamma]=
                            RASR[i_swath,iprf,i_gamma]
                      endelse

                endif
                endfor

          endfor

    endfor

    print, 'End of ASR estimations, Lets select optimum values of PRF'
    for iswath=swath_max, swath_min, -swathres do begin

          i_swath=(iswath-swath_min)/swathres
          for i_gamma=0, ngamma-1 do begin
                ;print, 'best PRF for look angle of ',
                i_gamma+min(gamma), '° & swath of',iswath, 'km'
                ilevel[i_swath,i_gamma]=0
                bestiprf=0
                for iprf=0,nprfpts-1 do begin
```

```
                        i_prf=(prfs[iprf]-min(prf))
                        if AMB_level[i_swath,i_prf,i_gamma] lt
                        ilevel[i_swath,i_gamma] then begin
                              ilevel[i_swath,i_gamma]=
                              AMB_level[i_swath,i_prf,i_gamma]
                              ;print, 'millor nivell pasem a ',
                              ilevel[i_swath,i_gamma],'dB'
                              BestPRFs[i_swath,i_gamma]=prfs[iprf]
                              bestiprf=i_prf
                              ;print, 'millor PRF
                              ',bestiprf+min(prf),'Hz'
                        endif
                  endfor
                  RASRbest[i_swath,i_gamma]=
                  RASR[i_swath,bestiprf,i_gamma]
                  RASRbest1[i_swath,i_gamma]=
                  RASR1[i_swath,bestiprf,i_gamma]
                  RASRbest2[i_swath,i_gamma]=
                  RASR2[i_swath,bestiprf,i_gamma]
                  AASRbest[i_swath,i_gamma]=
                  AASR[i_swath,bestiprf,i_gamma]
            endfor
      endfor
      if keyword_set(plot) then begin
            !P.BACKGROUND=0
            !P.COLOR=255
            if keyword_set(epsfile) then begin
                  SET_PLOT, 'PS'
                  DEVICE, FILENAME='minASR.ps'
            endif
            if keyword_set(paperstyle) then begin
                  !P.BACKGROUND=255
                  !P.COLOR=0
            endif
            !P.MULTI = 0
            plot,gammas, fltarr(ngamma)+asr_thres, xtitle="incidence
            angle (degrees)",ytitle="minimum ASR for each
            swath",xrange=[min(gammas), max(gammas)],yrange=[min(ilevel)-
            1,max(ilevel)]

            for k=0, nswaths-1 do begin

                  oplot,gammas,ilevel[k,*],LINESTYLE = k
                  ;stop
            endfor

            ;device,decomposed=0
            if keyword_set(epsfile) then begin
                  DEVICE, /CLOSE
                  SET_PLOT, 'win'
            endif

      endif

      return, {BestPRFs:BestPRFs,ASR:ilevel,gamma:gammas, AASR:AASRbest,
      RASR:RASRbest,RASR1:RASRbest1,RASR2:RASRbest2,ASR_mask:AASR_mask,
      Hanning_mask:hanning_mask, RASRall:RASR,AASRall:AASR}

end
```

7. bestLel

```
function bestLel, sar, GAMMA=GAMMA, SWATH_max=SWATH_max, PRF=PRF,
                  asr_thres=asr_thres, elbeam=elbeam, azbeam=azbeam,
                  nprfpts=nprfpts, plot=plot, epsfile=epsfile,
                  Lel_res=Lel_res, paperstyle=paperstyle,
                  Lel_min=Lel_min,Lel_max=Lel_max, L_az=L_az

      ;function to find the mínimum width that guarantie ambiguities
      requirements
      ;PRF: range of possible PRFs
      ;GAMMA: range of possible look angle values.
      ;SWATH: maximum swath wanted

      if not keyword_Set(GAMMA) then gamma=min(sar.gamma) ;look angle
      if not keyword_Set(swath_max) then swath_max=sar.swath
      if not keyword_Set(asr_thres) then asr_thres=-20
      if not keyword_Set(nprfpts) then nprfpts=100
      if not keyword_Set(Lel_res) then Lel_res=0.1
      if not keyword_Set(Lel_min) then Lel_min=Lel_res
      if not keyword_set(elbeam) then elbeam='uniform'
      if not keyword_set(azbeam) then azbeam='uniform'
      if not keyword_Set(Lel_max) then Lel_max=sar.L_el
      if not keyword_Set(L_az) then L_az=sar.L_az


      nLel=round((Lel_max-Lel_min)/Lel_res+1)

      ngamma=max(gamma)-min(gamma)+1
      gammas=findgen(ngamma+1)+min(gamma)


      nprfs=max(prf)-min(prf)
      prfs=round(min(prf)+(max(prf)-min(prf))*findgen(nprfpts)/(nprfpts))

      PRFvalid=fltarr(nprfs,ngamma)
      BestPRFs=fltarr(nLel,ngamma)
      RASR=fltarr(nLel, nprfs,ngamma)
      AASR=fltarr(nLel,nprfs,ngamma)
      AMB_level=fltarr(nLel,nprfs,ngamma)
      ilevel=fltarr(nLel,ngamma)
      RASRbest=fltarr(nLel,ngamma)
      AASRbest=fltarr(nLel,ngamma)


      PRFvalid=prfbad(sar,PRF=prf, GAMMA=GAMMA, SWATH=SWATH_max,plot=1) ;
      Non interference PRFs
      iLel=Lel_max
      for iLel=Lel_max, Lel_min,-Lel_res do begin
            i_Lel=(iLel-Lel_min)/Lel_res

            for i_gamma=0, ngamma-1 do begin

                  for i_prf=0,nprfpts-1 do begin

                        iprf=(prfs[i_prf]-min(prf))

                        if PRFvalid[iprf] ne 0 then begin ; valid PRF

                              AMB=saramb(sar, L_az=L_az, L_el=iLel,
                              PRF=PRFvalid[iprf, i_gamma], GAMMA=
```

```
                              gammas[i_gamma], SWATH=swath_max,
                              AASR=thisaasr, elbeam=elbeam,
                              azbeam=azbeam)
                              RASR[i_Lel,iprf,i_gamma]=db(max(AMB[*,1]))
                              AASR[i_Lel,iprf,i_gamma]=db(thisaasr)

                              if AASR[i_Lel, iprf,i_gamma] gt RASR[i_Lel,
                              iprf,i_gamma] then begin
                                    AMB_level[i_Lel,
                                    iprf,i_gamma]=AASR[i_Lel,
                                    iprf,i_gamma]
                              endif else begin
                                    AMB_level[i_Lel,
                                    iprf,i_gamma]=RASR[i_Lel,
                                    iprf,i_gamma]
                              endelse

                        endif
                  endfor

            endfor

      endfor



      for iLel=Lel_max, Lel_min,-Lel_res do begin
            i_Lel=(iLel-Lel_min)/Lel_res
            for i_gamma=0, ngamma-1 do begin
            ilevel[i_Lel,i_gamma]=0
                  bestiprf=0
                  for iprf=0,nprfpts-1 do begin

                        i_prf=(prfs[iprf]-min(prf))

                        if AMB_level[i_Lel,i_prf,i_gamma] lt
                        ilevel[i_Lel,i_gamma] then begin

                              ilevel[i_Lel,i_gamma]=
                              AMB_level[i_Lel,i_prf,i_gamma]
                              BestPRFs[i_Lel,i_gamma]=prfs[iprf]
                              bestiprf=i_prf

                        endif

                  endfor
                  RASRbest[i_Lel,i_gamma]= RASR[i_Lel,bestiprf,i_gamma]
                  AASRbest[i_Lel,i_gamma]= AASR[i_Lel,bestiprf,i_gamma]
            endfor
      endfor

      if keyword_set(plot) then begin
            !P.BACKGROUND=0
            !P.COLOR=255
            if keyword_set(epsfile) then begin
                  SET_PLOT, 'PS'
                  DEVICE, FILENAME='minASR.ps'
            endif
            if keyword_set(paperstyle) then begin
                  !P.BACKGROUND=255
```

```
            !P.COLOR=0
        endif
        !P.MULTI = 0
        plot,gammas, fltarr(ngamma)+asr_thres, xtitle="incidence
        angle (degrees)",ytitle="minimum ASR for each
        L_el",xrange=[min(gammas), max(gammas)], yrange=[min(ilevel)-
        1,max(ilevel)]

        for k=0, nLel-1 do begin

            oplot,gammas,ilevel[k,*],LINESTYLE = k
        endfor

        if keyword_set(epsfile) then begin
            DEVICE, /CLOSE
            SET_PLOT, 'win'
        endif

    endif

    return, {BestPRFs:BestPRFs,ASR:ilevel,gamma:gammas, AASR:AASRbest,
    RASR:RASRbest}

end
```

8. Other functions

```
function nbits, sar,grg_res=grg_res, az_res=az_res, F=F, Tant=Tant,
            h_sar=h_sar, Gamp=Gamp,ADCrange=ADCrange, DCnbits=ADCnbits,
            sigma_noise=sigma_noise, gamma=gamma, f0=f0, swath=swath,
            eta_ant=eta_ant, P_avg=P_avg, L_el=L_el, L_az=L_az,
            ap_eff=ap_eff, PRF=PRF, tau_p=tau_p, P_t=P_t


      if not keyword_set(grg_res) then grg_res=sar.grg_res
      if not keyword_set(az_res) then az_res=sar.az_res
      if n_elements(F) eq 0 then F=7.
      if not keyword_Set(f0) then f0=sar.f0
      if not keyword_set(h_sar) then h_sar=sar.h_sar
      if not keyword_set(L_el) then L_el=sar.L_el
      if not keyword_set(Tant) then Tant=300
      ;if not keyword_set(sigma_noise) then sigma_noise=sar.sigma_noise
      if not keyword_set(gamma) then gamma=min(sar.gamma)
      if not keyword_Set(eta_ant) then eta_ant=sar.eta_ant
      if not keyword_Set(ap_eff) then ap_eff=sar.ap_eff


      ;;constants
      c=3e8                           ;Speed of light
      j=complex(0,1)
      kb=1.38e-23      ;Boltzman constant
      To=290

      R_earth=6371e3
      R_s=6371e3 + h_sar          ;From earth-center to sensor
      R_t=6371e3                    ;From earth-center to targe

      ;;derived constants
      lambda_0=c/f0                   ;Carrier wavelength
      k_0=2*!pi/lambda_0
      ;; Look angle
      gamma_1=!dtor*min(gamma)
      eta_c1=asin(R_s/R_t*sin(gamma_1)) ;Boresight incidence angle

      ;;Lets calculate the necessary bandwidth
      srg_res=grg_res*sin(eta_c1)  ;Slant-range resolution

      ;;Therefore the chirp bandwidth is
      ;; srg_res=c/(2*NBW)
      Bn=c/2/srg_res
      R_1=R_s*cos(gamma_1)-sqrt(R_t^2-R_s^2+R_s^2*cos(gamma_1)^2) ;From
      sensor to target
      ;;From the azimuth resolution we can derive the antenna length in

      if not keyword_Set(L_az) then begin
            ;;stripmap mode
            L_az=2*az_res
      endif
      ;;we can correct it by a spotlight factor...
      ;;azimuth beamwidth
      gamma_az=lambda_0/L_az

      ;;Doppler bandwidth
      v_orb=orbit_vel(h_sar)
      B_dop=v_orb*gamma_az*2/lambda_0
      PRFmin=B_dop
```

```
	PRTmax=1./PRFmin
	Ramb=c/2*PRTmax
	;;Non ambiguous swath:

	if not keyword_Set(swath) then begin
		;;If swath is not specified then set to max unambigous
		swath=Ramb/sin(eta_c1)
	endif

	G_t=ap_eff*4*!PI*(L_el/lambda_0)*(L_az/lambda_0)
	if not keyword_Set(P_t) then begin
		P_t=P_avg/tau_p/PRF
	endif

	Fsys=Tant/To+(db2lin(F)-1)

	if not keyword_Set(sigma_noise) then begin
		;supose sigma_noise 0dB due to a brilliant distributed target

		sigma_noise=1 ;0dB
	endif

	theta_h=lambda_0/L_az

	;;                Pt.Gt^2.lambda_0^2.sigma_noise.theta_h.c.tau_p
	;; SNRo = ---------------------------------------------------
	;;                   2.(4*!PI.R)^3.kb.To.Fsys.Bn.sin(eta_c1)

	SNR=(P_t*G_t^2*lambda_0^2*sigma_noise*theta_h*c*tau_p)/(
	2*(4*!pi*R_ 1)^3*To*kb*Fsys*Bn*sin(eta_c1))
	N=(db(SNR)-1.8)/6
	print, (N), 'bits'


	t_obs=2*swath*sin(eta_c1)/c+tau_p
	F_s=2*Bn
	bit_rate=t_obs*F_s*PRF*ceil(N)


	;;Return bits number, SNR, t_obs , bit rate
	res=[[N],[db(SNR)],[t_obs],[bit_rate]]
	return, res

end


function sinc,x
	if n_elements(x) eq 1 then begin
		if x eq 0 then return, 1 else return, sin(!pi*x)/(!pi*x)
	endif else begin
		nozeros=where(x ne 0,num_nozero)
		res=x*0+1
		if num_nozero gt 0 then res[nozeros]=sin(!pi*x[nozeros])/
		(!pi*x[nozeros])
	return,res
	endelse


end
```

```
function sincbp, theta, La,f0,field=field

      ;;Function to calculate a 1-d one dimesional patter for a uniform
      ilumination
      c=3e8
      lambda=c/f0
      k0=2*!pi/lambda
      u=sin(theta)

      if keyword_set(field) then begin
            return, sinc(La*u/lambda);/(La*u/lambda) ;;sinc!!!!!!!!
      endif else return,(sinc(La*u/lambda))^2

end

function circbp, theta, ra,f0,field=field
      ;;Function to calculate a 1-d one dimesional patter for a uniform
      ilumination
      c=3e8
      lambda=c/f0
      k0=2*!pi/lambda
      z=k0*ra*sin(theta)
      e= beselj(z,1)/z
      bad=where(z eq 0,nbad)
      if nbad ge 1 then e[bad]=0
      if keyword_set(field) then begin
            return, e
      endif else return, (e)^2

end

function hanningbp, theta, La,f0,field=field
      ;;Function to calculate a 1-d one dimesional patter for a uniform
      ilumination
      c=3e8
      lambda=c/f0
      k0=2*!pi/lambda
      u=sin(theta)
      npts=2048*8
      ipts=512
      oversamp=npts*1.0/ipts
      ilum=[hanning(ipts),fltarr(npts-ipts)]
      bp=fft(ilum)
      ;;if keyword_set(field) then begin
      ;;   return, sinc(La*u/lambda)
      ;;endif else return, (sinc(La*u/lambda))^2
      g0=abs(bp[0])^2
      ;;g=abs(bp(round(abs(oversamp*La*u/lambda))))^2
      g=abs(interpolate(bp,abs(oversamp*La*u/lambda)))^2
      return, g/g0

end
```

```
function db, data,norm=norm
      on_error,2
      if keyword_set(norm) then begin
            tmp=10*alog10(abs(data))
            return, tmp-max(tmp)
      endif else begin
            return, 10*alog10(abs(data))
      endelse
end


function db2lin, in, amp=amp
      if keyword_set(amp) then begin
            return, 10.^(in/20.0)
      endif else begin
            return, 10.^(in/10.0)
      endelse

end
```